

ZO-1 controls endothelial adherens junctions, cell–cell tension, angiogenesis, and barrier formation

Olga Tornavaca,¹ Minghao Chia,¹ Neil Dufton,⁴ Lourdes Osuna Almagro,⁴ Daniel E. Conway,⁵ Anna M. Randi,⁴ Martin A. Schwartz,^{2,3} Karl Matter,^{1*} and Maria S. Balda^{1*}

¹Department of Cell Biology, UCL Institute of Ophthalmology, University College London, London EC1V 9EL, England, UK

²Department of Medicine and ³Department of Cell Biology, Yale University, New Haven, CT 06520

⁴National Heart and Lung Institute (NHLI) Vascular Sciences Unit, Imperial Centre for Translational and Experimental Medicine (ICTEM), Hammersmith Hospital, Imperial College London, London W12 0NN, England, UK

⁵Department of Biomedical Engineering, Virginia Commonwealth University, Richmond, VA 23284

Intercellular junctions are crucial for mechanotransduction, but whether tight junctions contribute to the regulation of cell–cell tension and adherens junctions is unknown. Here, we demonstrate that the tight junction protein ZO-1 regulates tension acting on VE-cadherin-based adherens junctions, cell migration, and barrier formation of primary endothelial cells, as well as angiogenesis *in vitro* and *in vivo*. ZO-1 depletion led to tight junction disruption, redistribution of active myosin II from junctions to stress fibers, reduced tension on VE-cadherin and loss of junctional mechanotransducers such as vinculin and

PAK2, and induced vinculin dissociation from the α -catenin–VE-cadherin complex. Claudin-5 depletion only mimicked ZO-1 effects on barrier formation, whereas the effects on mechanotransducers were rescued by inhibition of ROCK and phenocopied by JAM-A, JACOP, or p114RhoGEF down-regulation. ZO-1 was required for junctional recruitment of JACOP, which, in turn, recruited p114RhoGEF. ZO-1 is thus a central regulator of VE-cadherin-dependent endothelial junctions that orchestrates the spatial actomyosin organization, tuning cell–cell tension, migration, angiogenesis, and barrier formation.

Introduction

Endothelial cells (EC) cover the internal surface of blood and lymphatic vessels, and play key roles in vessel formation and function. Regulation of endothelial cell–cell junctions is critically important in inflammation and angiogenesis, and incorrect junctional permeability is a major contributing factor to morbidity and mortality in acute lung injury and sepsis (Weber et al., 2007; Haskard et al., 2013). EC homeostasis requires the integration of signals from sites of adhesion to the extracellular matrix and neighboring cells, as well as signals from circulating factors and mechanical stimuli. We are only starting to understand how these different types of signals influence each other and how they impact endothelial behavior and function (Cavallaro and Dejana, 2011; Pulimeno et al., 2011). The integration, transmission, and regulation of mechanical forces at sites of adhesion is of fundamental importance, as they drive vessel development and progression of diseases such as atherosclerosis and hypertension (Conway and Schwartz, 2012).

Intercellular tight junctions are crucial for the formation of endothelial barriers, as they regulate paracellular diffusion. They have also been linked to angiogenesis and polarization, and their composition and integrity are affected by carcinogenesis and inflammation (Bazzoni, 2011; Martin, 2014). Tight junctions are composed of different types of transmembrane proteins and a complex set of cytosolic proteins that link the junctional membrane to the cytoskeleton to regulate endothelial barrier function (Lampugnani, 2012). Tight junction transmembrane proteins in EC include claudin-5, occludin, and several JAMs. Claudin-5 is a critical determinant of blood–brain barrier permeability in mice (Nitta et al., 2003), and JAM family adhesion proteins have been linked to angiogenesis, migration, and crosstalk with FGF-2 and α v β 3 integrin signaling (Lamagna et al., 2005; Cooke et al., 2006; Severson et al., 2009; Peddibhotla et al., 2013).

ZO-1 is a junctional adaptor protein that interacts with multiple other junctional components, including the transmembrane

*K. Matter and M.S. Balda contributed equally to this paper.

Correspondence to Maria S. Balda: m.balda@ucl.ac.uk

Abbreviations used in this paper: EC, endothelial cells; HDMEC, human dermal microvascular EC; MC, microcarrier.

© 2015 Tornavaca et al. This article is distributed under the terms of an Attribution–Noncommercial–Share Alike–No Mirror Sites license for the first six months after the publication date (see <http://www.rupress.org/terms>). After six months it is available under a Creative Commons License (Attribution–Noncommercial–Share Alike 3.0 Unported license, as described at <http://creativecommons.org/licenses/by-nc-sa/3.0/>).

proteins of the claudin and JAM families (Bazzoni et al., 2000; Ebnet et al., 2000; Fanning and Anderson, 2009). The relevance of such interactions for the localization and function of the binding partners is not well understood, largely because of a lack of clear phenotypes in the analyzed epithelial model systems due to functional redundancy with ZO-2. Similarly, ZO-1 binds F-actin and has been linked to the regulation of the actomyosin cytoskeleton; however, the reported results from epithelia are contradictory, and it is not clear whether ZO-1 is important for overall actomyosin function (Yamazaki et al., 2008; Van Itallie et al., 2009; Fanning et al., 2012). This contrasts with EC, as ZO-1 knockout mice are embryonic lethal (embryonic day 9.5–10.5) and ZO-1 is required for normal blood vessel formation in the yolk sac, which suggests that ZO-1 may be functionally important for endothelial tissue organization. However, the underlying cellular and molecular mechanisms for ZO-1's importance for vessel formation in the yolk sac, and its effect on endothelial permeability are not known (Katsuno et al., 2008).

Here, we asked whether ZO-1 is important for endothelial integrity and function in primary human dermal microvascular EC (HDMEC) and whether it regulates angiogenic properties of EC. Our results demonstrate that ZO-1 indeed regulates angiogenesis *in vitro* and *in vivo*, and is essential for endothelial barrier formation, spatial actomyosin organization, and cell–cell tension as well as cell migration. Our data indicate that different junctional membrane proteins that bind ZO-1 serve distinct purposes, with JAM-A forming a cooperative unit with ZO-1 and claudin-5 functioning as a downstream effector required for barrier formation. We demonstrate that ZO-1 regulates recruitment of mechanotransducers to the VE-cadherin complex via the recruitment of a junctional regulatory complex containing JACOP and the RhoA activator p114RhoGEF, and, thereby, junctional tension. Our data thus establish a molecular regulatory network by which tight junctions regulate adherens junctions and endothelial behavior and function.

Results

ZO-1 regulates endothelial cell–cell tension

We established a loss-of-function approach to determine the role of ZO-1 in EC using HDMEC. HDMEC were chosen because we found them to form robust and regular junctional complexes. Two distinct siRNAs were identified that effectively down-regulated ZO-1 (Fig. 1, A and B).

ZO-1 is thought to regulate the actomyosin cytoskeleton in epithelial cells; however, its function remains controversial, as depletion was linked to both increased and decreased junctional actomyosin (Yamazaki et al., 2008; Van Itallie et al., 2009; Fanning et al., 2012). We thus asked whether depletion of ZO-1 had an effect on the recruitment and activity of junctional actomyosin in EC. In control HDMEC, β -actin and myosin IIA formed a junctional belt that was positive for double phosphorylated myosin light chain 2 (MLC2), which indicates that myosin was active (Fig. 1 C). Upon depletion of ZO-1, both myosin IIA and β -actin redistributed and formed stress fibers along the base of the cells that were also positive for double-phosphorylated MLC2. By immunoblotting, the levels of doubly phosphorylated

MLC2 were increased, whereas single phosphorylated MLC2 levels remained similar (Fig. 1 D). When mouse GFP-tagged ZO-1 was expressed in the ZO-1–depleted human EC, junctional localization of myosin was rescued and formation of stress fibers was repressed, which indicates that the observed phenotype in depleted cells was specific (Fig. 1 E). Loss of ZO-1 thus induced a reorganization of the actomyosin cytoskeleton.

We next asked whether these changes resulted in altered tensile force on the junctional complex. We used a FRET biosensor based on VE-cadherin that carries an elastic force sensor within the cytoplasmic domain between the p120 and the β -catenin binding sites (Grashoff et al., 2010; Conway et al., 2013). Fig. 2 (A and B) shows that the sensor was sensitive to the presence of the β -catenin binding site, which indicates that the probe responded to forces that act on VE-cadherin. Depletion of ZO-1 also led to increased FRET efficiency, indicating that the tensile force acting on VE-cadherin was diminished (Fig. 2, A and B). Therefore, reduced ZO-1 expression stimulated a reduction in the tension on VE-cadherin, which suggests that ZO-1 regulates tension on adherens junctions.

We next determined whether reduced tension on VE-cadherin indeed translated into reduced tension of endothelial cell–cell contacts using laser ablation. HDMEC were infected with a lentiviral vector encoding GFP– α -catenin to mark cell–cell boundaries and were then transfected with siRNAs. In control cells, ablation of a cell led to a contraction of neighboring cells and extension of the surface covered by the ablated cell (Fig. 2 C and Video 1). In ZO-1–depleted cells, both extension of the ablated cell and contraction of neighboring cells were reduced by >60% (Fig. 2, C–E; and Video 2). Hence, ZO-1 regulates tension on endothelial cell–cell contacts.

Our data thus indicate that ZO-1 is an essential orchestrator of endothelial spatial actomyosin organization and regulates the tensile force acting on adherens junctions.

ZO-1 regulates endothelial cell migration and angiogenic potential

Angiogenesis requires complex actin reorganization and migration of EC to generate functional new vessels. Hence, we asked whether ZO-1 regulates the angiogenic potential of EC. We first used a migration assay to determine if ZO-1 affected collective cell migration. Fig. 3 (A and B) shows that cells lacking normal ZO-1 expression migrated less. An *in vitro* Matrigel tubulogenesis assay further revealed that ZO-1 depletion led to reduced network formation *in vitro* (Fig. S1, A and B). ZO-1 depletion was also found to reduce endothelial sprouting in a 3D microcarrier (MC)-based fibrin gel angiogenesis assay (Fig. 3, C–E). ZO-1 thus regulates the angiogenic potential of HDMEC primary cultures.

Next, we tested whether ZO-1 down-regulation inhibited angiogenesis *in vivo*. To suppress ZO-1 expression in mouse, we designed and tested specific mouse siRNAs (Fig. S1 C). Two of these siRNAs were then used in *in vivo* angiogenesis experiments using the Matrigel plug model (Birdsey et al., 2008). A Matrigel mixture containing siRNA, heparin, and basic FGF was injected subcutaneously into C57BL/6 mice. After 7 d, plugs were harvested and analyzed (Figs. 3 F and S1, D and E).

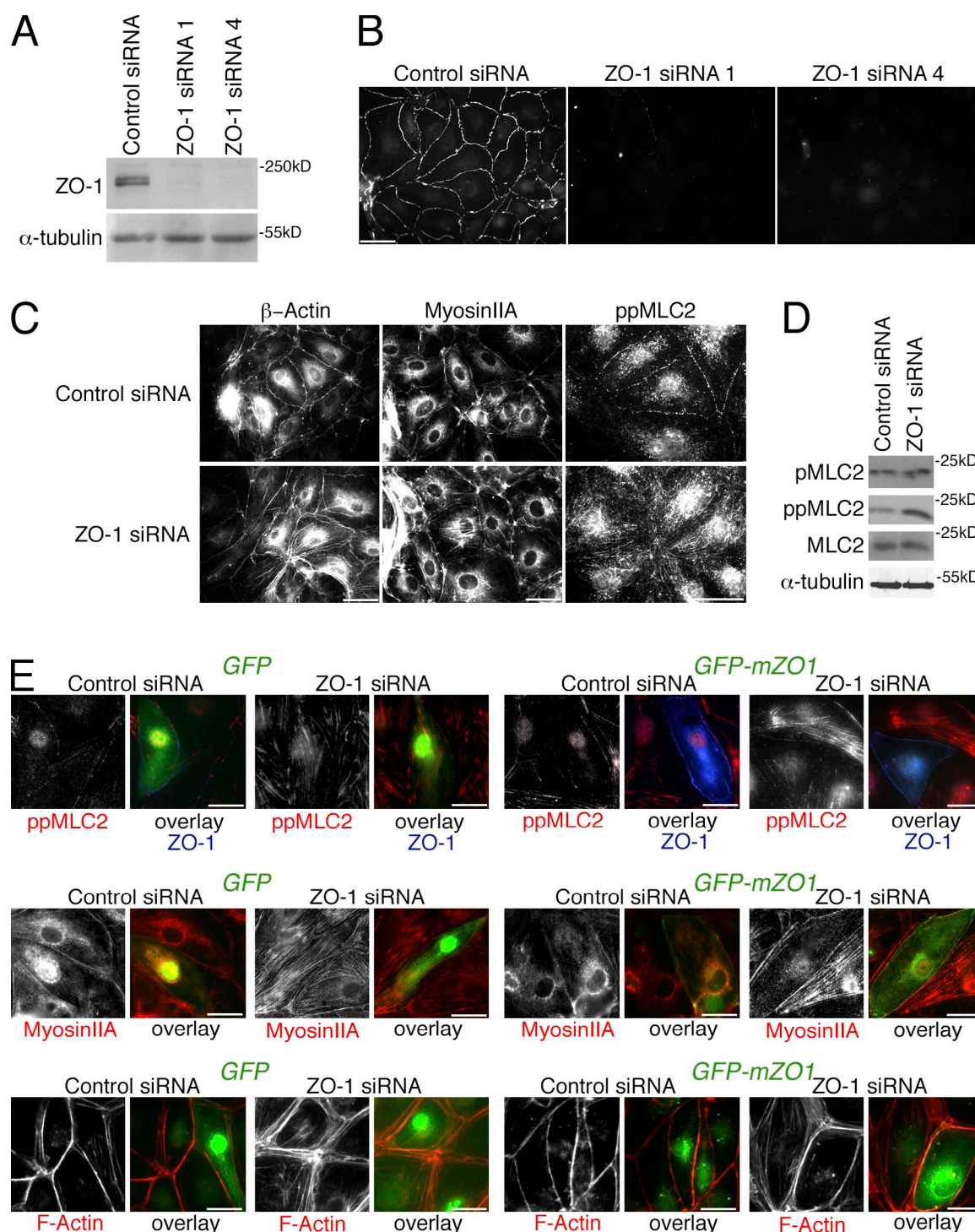
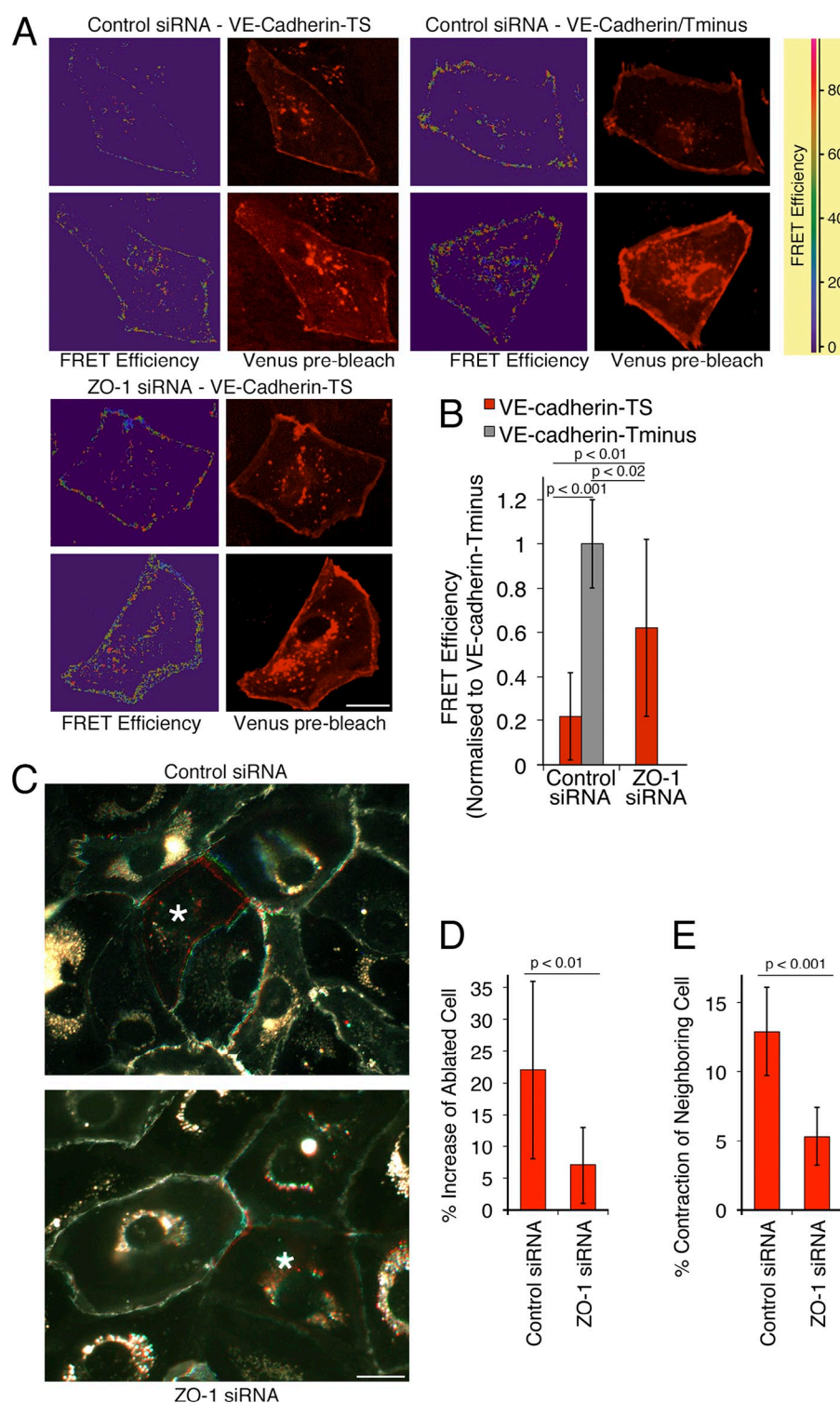


Figure 1. ZO-1 regulates the endothelial actomyosin distribution. (A–C) Cells transfected with nontargeting (Control) siRNA or siRNAs directed against ZO-1 were analyzed by immunoblotting for ZO-1 and α -tubulin expression (A), or processed for immunofluorescence microscopy using antibodies against ZO-1 (B) or β -actin, myosin IIA, or double-phosphorylated MLC2 (C). (D) Cells transfected with siRNAs were analyzed by immunoblotting for single- and double-phosphorylated, as well as total, MLC2, and, as a loading control, α -tubulin. (E) Cells that had been transfected with siRNAs as indicated were additionally transfected with GFP or GFP-mZO1, a fusion protein constructed with a mouse ZO-1 cDNA, 24 h before analysis. The cells were then fixed and stained as indicated to monitor loss of stress fibers and increased junctional staining of F-actin and myosin upon ZO-1 reexpression. Bars: (A–C) 40 μ m; (E) 20 μ m.

Immunofluorescence revealed that ZO-1 expression was reduced with ZO-1-specific siRNAs in the sections of the plugs (Fig. S1 D). Quantification of blood vessels by hematoxylin and eosin staining revealed that FGF strongly stimulated vessel growth, as

expected. Whereas control siRNAs did not significantly affect the angiogenic response to FGF, ZO-1 siRNAs reduced the vessel number by $\sim 50\%$ (Fig. 3, F and G; and Fig. S1 E). Hence, ZO-1 also regulates angiogenesis in an in vivo mouse model.

Figure 2. ZO-1 down-regulation reduces endothelial cell-cell tension. (A and B) Cells were transfected with siRNAs and, after 2 d, with a VE-cadherin-based FRET tension sensor containing (TS) or lacking (Tminus) the β -catenin binding site. FRET activity was then imaged by gain of donor fluorescence after acceptor bleaching from confluent monolayers. (A) FRET efficiency maps and images taken from venus fluorescent protein before bleaching. (B) Images were quantified by calculating the FRET efficiencies at cell-cell contacts. The values were then normalized to the FRET efficiency obtained with the tail-minus construct, which does not sense tension and hence provides the FRET signals that can maximally be expected (shown are means \pm 1 SD [error bars]; $n = 12$). (C–E) Cells expressing GFP- α -catenin were plated and transfected with siRNAs as in A. The cells were then analyzed by ablating single cells (marked with an asterisk) within the monolayer with a laser and recording the movement of cell-cell contacts in the GFP channel for 1 min. The images in C show overlays of frames taken before ablation in red, after 30 s in green, and after 45 s in blue (see also Videos 1 and 2). The increase in the surface area of the ablated cells and the contraction of the neighboring cells were then analyzed (D and E, shown are means \pm 1 SD [error bars]; $n = 11$). Bars, 20 μ m.



These data show that ZO-1 is not only crucial for cortical actomyosin function but regulates endothelial cell migration and angiogenesis.

ZO-1 depletion leads to a selective loss of tight junction proteins and mechanotransducers

To identify the molecular consequences of ZO-1 depletion, we next asked whether ZO-1 is required for the recruitment of

junctional proteins and mechanotransducers to cell-cell contacts. Depletion of ZO-1 led to reduced junctional recruitment of two crucial transmembrane components of tight junctions: claudin-5 and JAM-A (Fig. 4, A and B). Claudin-5 was also expressed at lower levels at least in part due to lysosomal degradation (Fig. S2 A). In contrast, localization of ZO-2, which is thought to function redundantly with ZO-1, was not affected. These experiments therefore identify a ZO1-specific function in EC that is not shared with ZO-2.

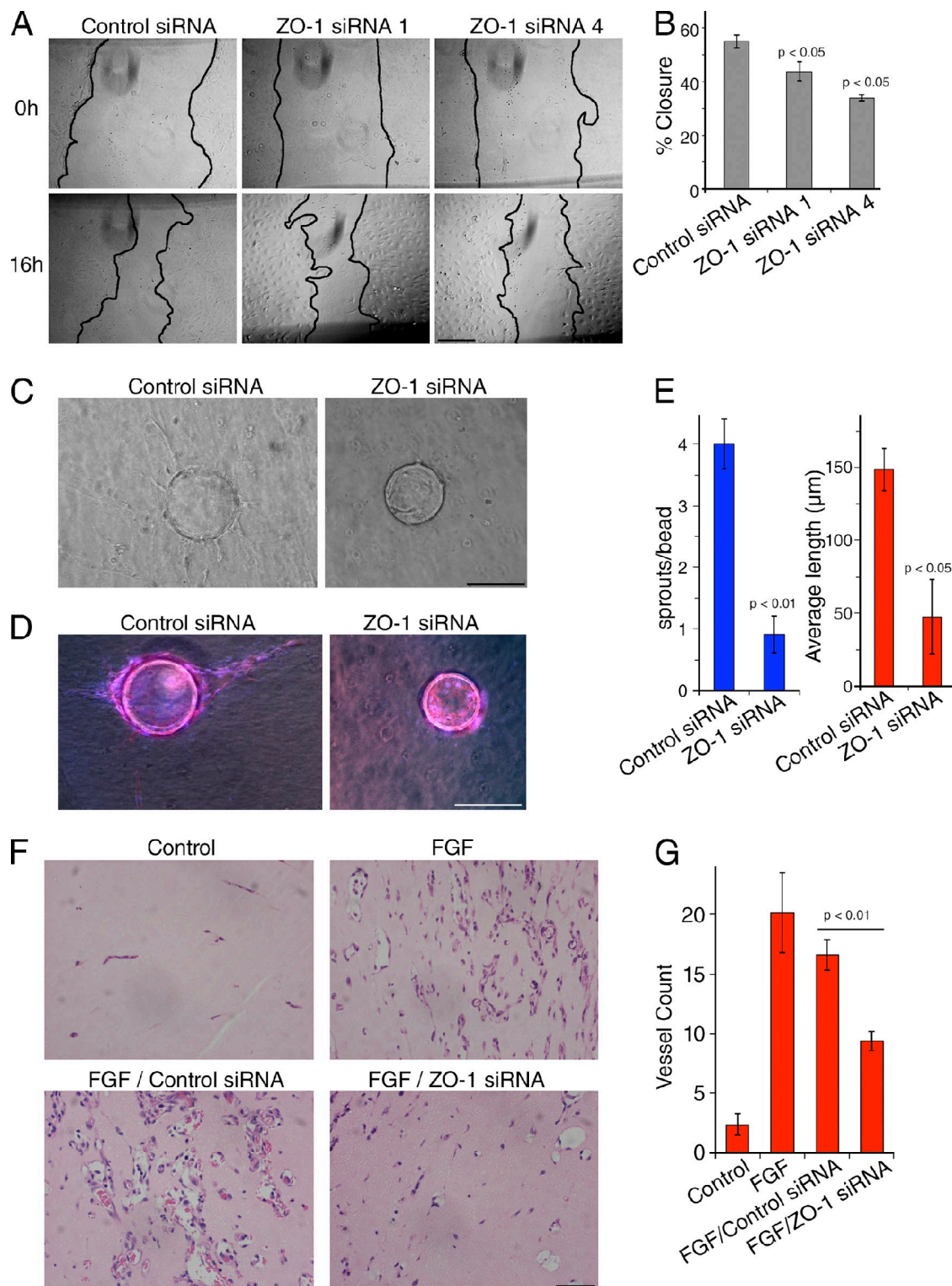


Figure 3. ZO-1 down-regulation reduces endothelial cell migration and angiogenic potential. (A) HDMEC were transfected with the indicated siRNAs for 48 h. Scratch wounds were then inflicted to induce cell migration. Representative images of wounds are shown that were taken at 0 and 16 h after scratching. (B) Percentages of the areas of closure of three independent experiments; shown are means \pm 1 SD [error bars]. (C–G) The effect of the depletion of ZO-1 on endothelial angiogenic potential was tested in vitro using an MC-based fibrin gel angiogenesis assay (C–E) or Matrigel plugs in vivo (F and G). For in vitro assays, HDMEC were seeded onto beads 24 h after siRNA transfection and were then embedded in a 3D fibrin gel after another 24 h. (C) Sprouting was then analyzed after 4 d by phase-contrast microscopy. (D) The cells were then fixed, permeabilized, and stained for nuclei (blue) and F-actin (red) to monitor coverage of beads with cells. (D and E) The number of sprouts per bead (D) and the mean length (E) were then determined (shown are means \pm 1 SD [error bars] of four experiments). (F and G) For in vivo assays, mice were injected with Matrigel-containing FGF and siRNAs as indicated to induce angiogenesis. After 7 d, the plugs were harvested and fixed, embedded in paraffin, and sectioned. Sections in E were stained by hematoxylin and eosin, and were used to quantify the number of vessels shown in F (shown are means \pm 1 SD [error bars]; control and FGF, n = 6; siRNA samples, n = 12). Bars, 250 μ m.

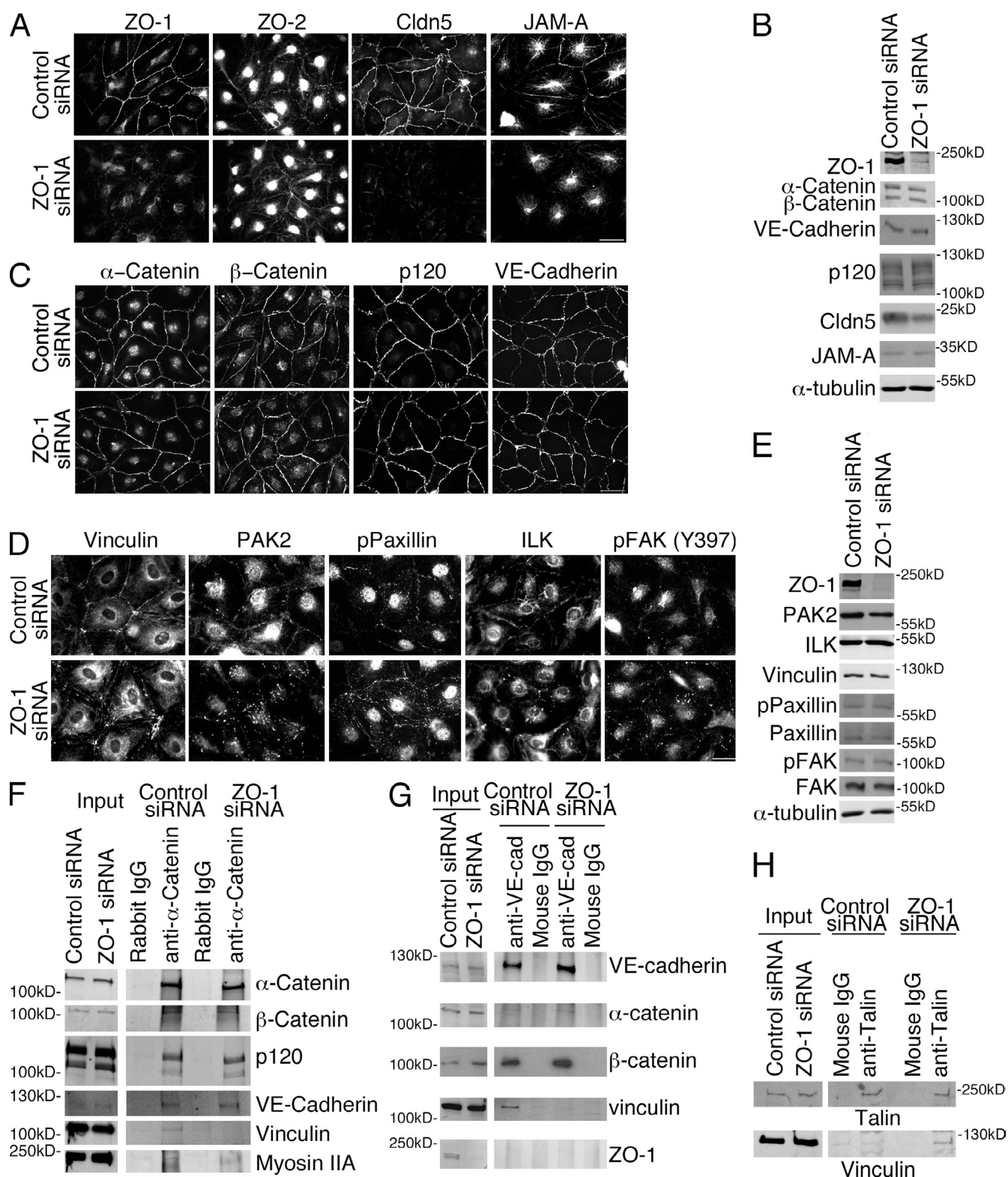


Figure 4. ZO-1 depletion leads to a selective redistribution of tight junction proteins and junctional mechanotransducers. (A–E) HDMEC with or without down-regulation of ZO-1 were analyzed by immunofluorescence and immunoblotting using antibodies for the indicated tight junction (A and B) and adherens junction (B and C) proteins, as well as mechanotransducers and regulators (D and E). (F–H) Control and siRNA-depleted cells were extracted and used for immunoprecipitation with antibodies against α -catenin (F), VE-cadherin (G), or talin (H). Immunoprecipitates were then analyzed by immunoblotting as indicated. Results shown are representative from three duplicate experiments. Bars: (A) 40 μ m; (C) 50 μ m; (D) 30 μ m.

The biosensor and ablation experiments indicated that depletion of ZO-1 led to reduced tensile force on VE-cadherin-based junctions; hence, we examined the distribution of the cadherin and associated catenins. However, neither the localization nor the total expression levels of VE-cadherin, α - and β -catenin, or p120catenin were noticeably affected (Fig. 4, B and C). Because down-regulation of ZO-1 affected cell–cell tension, we next examined localization and expression of vinculin, which shows force-dependent association with endothelial VE-cadherin junctions by binding to α -catenin (Grashoff et al., 2010; Yonemura et al., 2010; Huveneers et al., 2012). Fig. 4 (D and E) shows that ZO-1 down-regulation triggered redistribution of vinculin from cell–cell junctions to focal adhesions, mirroring the changes in active myosin shown in Fig. 1. Expression of GFP-tagged mouse ZO-1 rescued the junctional localization of vinculin in depleted cells (Fig. S2 B). Depletion of ZO-1 also led to a selective loss of vinculin from immunoprecipitated α -catenin and VE-cadherin complexes and increased coprecipitation with the focal adhesion protein talin (Fig. 4, F–H), which supports the conclusion that ZO-1 regulates the recruitment of the force-generating and transducing machinery to VE-cadherin-based junctions.

The redistribution of vinculin in ZO-1-depleted cells suggested that the molecular complex that couples and regulates actomyosin-generated forces to sites of adhesion may have been redistributed along with myosin IIA; hence, we tested other components of this supramolecular assembly. PAK2 and phospho-paxillin were enriched at cell–cell junctions in control cells, but concentrated in focal adhesions in ZO-1-depleted cells (Fig. 4 D). Staining for ILK and activated FAK at focal adhesion was also pronounced in response to ZO-1 depletion (Fig. 4 D).

The data thus far indicate that ZO-1 orchestrates the spatial distribution of major components of adhesive complexes that regulate force generation and transmission at cell–cell junctions and focal adhesions, with significant consequences for cell–cell tension, migration, and angiogenesis.

Loss of Claudin-5 regulates barrier function

Claudin-5 is a component of junctional intramembrane strands and a critical determinant of blood–brain barrier permeability in mice (Nitta et al., 2003); hence, we asked whether its disappearance from cell junctions is relevant for the defect in cell–cell tension, migration, and angiogenesis induced by ZO-1 depletion (Fig. 4, A and B).

siRNAs targeting claudin-5 induced efficient depletion of the protein and a strong increase in transendothelial permeability, indicating that the endothelial barrier was compromised (Fig. S2, C–G). There were no differences in cell numbers, necrosis, or apoptosis, which indicates that the increase in permeability was due to defects in the paracellular diffusion barrier (unpublished data). As the increase in paracellular diffusion was comparable to what we observed upon ZO-1 depletion, loss of junctional claudin-5 in ZO-1-depleted cells is sufficient to explain the barrier defect. In contrast, claudin-5 depletion affected neither junctional and cytoskeletal markers nor tubulogenesis and migration (Fig. S2). Therefore, depletion of claudin-5 led to

a selective defect in the endothelial permeability barrier and not other phenotypic changes induced by ZO-1 depletion.

Loss of JAM-A induces disorganization of ZO-1 and claudin-5

JAM-A regulates endothelial cell migration and angiogenesis, as it influences both FGF-2 and $\alpha v \beta 3$ integrin signaling (Nehls and Drenckhahn, 1995; Lamagna et al., 2005; Cooke et al., 2006; Severson et al., 2009; Peddibhotla et al., 2013). Therefore, we next asked whether the second tight junction protein affected by ZO-1 depletion (Fig. 4, A and B) is important for cytoskeletal rearrangement.

JAM-A was efficiently depleted by two siRNAs and affected the localization of claudin-5 and ZO-1, but not VE-cadherin (Fig. 5). Hence, JAM-A and ZO-1 appear to be linked in a bidirectional, cooperative manner, as each influenced the other's distribution and both were required for claudin-5 localization at tight junctions. Reduced expression of JAM-A induced redistribution of PAK2 and vinculin from cell contacts to focal adhesions and induction of stress fibers (Fig. 5 C). ZO-1 and JAM-A therefore form a functional unit that regulates tight junction assembly and cytoskeletal organization.

Loss of PAK2 stimulates reorganization of the cytoskeleton

Depletion of ZO-1 and JAM-A stimulated a striking reorganization of the actin cytoskeleton. Among the cytoskeletal proteins affected was PAK2, which has been observed to regulate endothelial contractility and junctional integrity (Stockton et al., 2004). Depletion of PAK2 had a striking effect on junction morphology (Fig. 6, A and B). Although ZO-1 and claudin-5 remained junctional, their distribution was partially disrupted and irregular. VE-cadherin became irregular and did not form linear junctions anymore. PAK2 is thus critical for the normal organization of tight and adherens junctions.

We next assayed effects on the actomyosin cytoskeleton. Myosin IIA became redistributed and stress fibers were induced in response to PAK2 depletion in a similar manner to when ZO-1 was depleted (Figs. 1 C and 6 C). Vinculin also disappeared from cell–cell contacts and associated with the prominent focal adhesions induced by PAK2 depletion. Phosphorylated MLC2 was lost from junctions and became more enriched along basal actin fibers (Fig. 6, C and D). Hence, PAK2 depletion led to a similar reorganization of the actin cytoskeleton as ZO-1 or JAM-A depletion, which indicates that the loss of junctional PAK2 in ZO-1- or JAM-A-depleted cells is functionally relevant and that the kinase is required for the maintenance of endothelial junctions. ZO-1 and claudin-5 were still junctional, which indicates that PAK2 functions downstream of ZO-1.

Balance of myosin activation maintains the junctional complex

Depletion of ZO-1 or JAM-A led to a loss of junctional myosin IIA in favor of stress fibers. This was paralleled by an analogous redistribution of vinculin; hence, we speculated that the reorganization of the cytoskeleton and the deformation of cell junctions was caused by an imbalance of myosin-generated

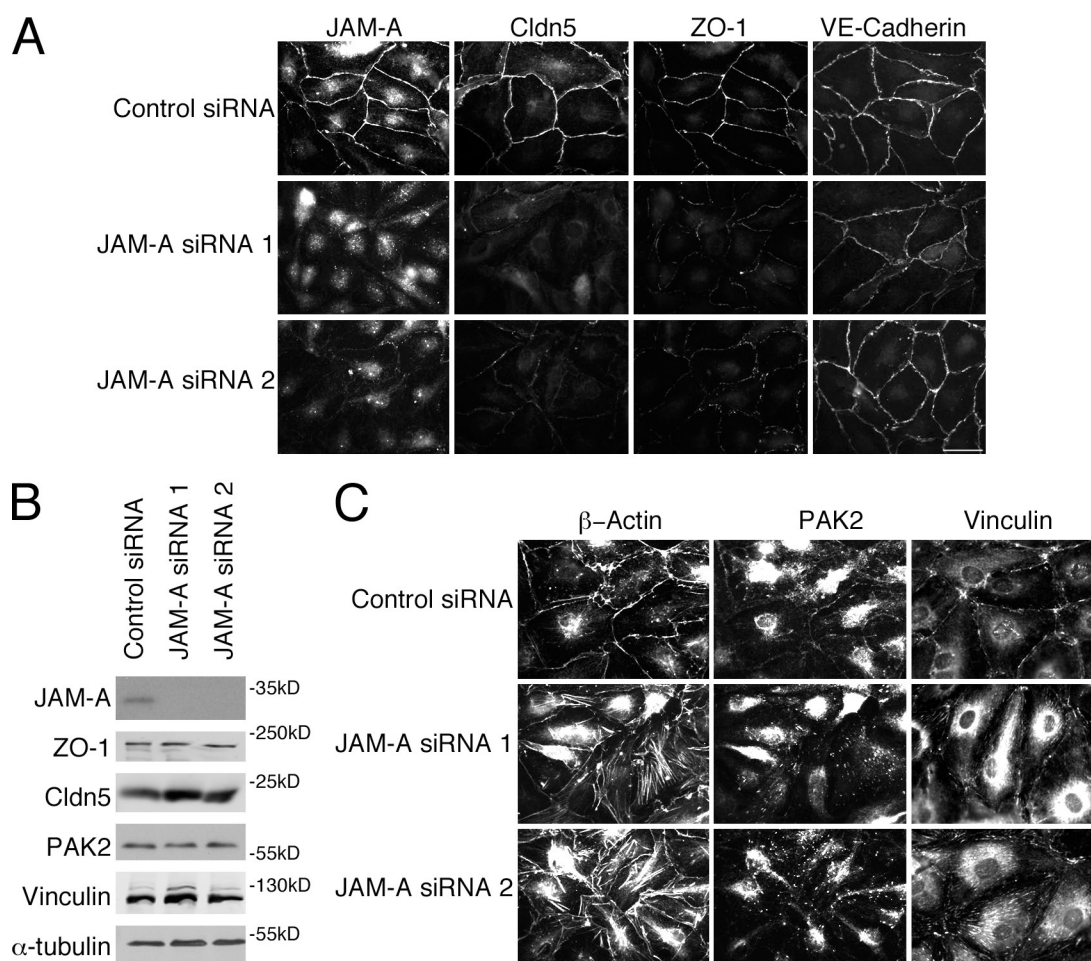


Figure 5. **JAM-A down-regulation redistributes ZO-1 and claudin-5, and induces focal adhesions.** (A and C) Cells transfected with control or JAM-A siRNAs were analyzed by immunofluorescence for the indicated proteins. (B) Equivalent samples were analyzed by expression of the indicated proteins by immunoblotting. Results shown are representative from three duplicate experiments performed. Bars, 30 μ m.

subcellular tension distribution. To test this, we tested the ability of ROCK inhibition to block myosin activation.

ROCK inhibition had a striking effect on the siRNA-induced phenotypes (Fig. 7). Junctional proteins that had been lost in response to ZO-1 or JAM-A depletion accumulated again at cell–cell contacts (only localization, not expression levels of claudin-5 were recovered; unpublished data). Myosin IIA, β -actin, and vinculin increased at cell–cell junctions, whereas focal adhesions and stress fibers disappeared. There was also recruitment of PAK2; however, junctional phosphorylated MLC2 remained low in ZO-1–depleted cells in the presence of the ROCK inhibitor (unpublished data).

ROCK is activated by RhoA signaling. Hence, we tested whether ZO-1 depletion affected the distribution of active RhoA using a biosensor. Fig. S3 shows that ZO-1 depletion led to reduced RhoA activity at cell–cell contacts, whereas activity in the rest of the cells increased.

These data thus indicate that the endothelial phenotype is maintained by a balance between myosin-generated tension at cell–cell and cell–matrix contacts, and that ZO-1 and JAM-A are required to maintain junctional actomyosin activity, possibly involving junctional recruitment of a RhoA regulator.

VE-cadherin functions upstream of ZO-1

The cadherins are generally thought to be the master organizers of cell–cell junctions; however, the data in EC on the role of VE-cadherin in the recruitment of tight junction components are conflicting. VE-cadherin could be efficiently depleted (Fig. 8 A), which strongly affected junctional recruitment of the core adherens junction components α - and β -catenin (Fig. 8 A). Actin and myosin IIA redistributed from junctions to stress fibers, vinculin and PAK2 redistributed to focal adhesions, and tight junctions were disrupted. ROCK inhibition did not rescue the disruption of α - and β -catenin, but ZO-1, claudin-5, and JAM-A relocalized to cell–cell junctions, stress fibers were reduced, and vinculin and PAK2 disappeared from focal adhesions (Fig. 8 C). These data indicate that VE-cadherin functions upstream of ZO-1 and is required for its recruitment in part through regulation of the actin cytoskeleton and myosin contractility. Together with the overlap in the phenotypes, this suggests that ZO-1 is an integral component of the regulatory mechanisms that are activated by VE-cadherin to stimulate endothelial junction formation and mediates reorganization of the actin cytoskeleton to form functional endothelial junctions.

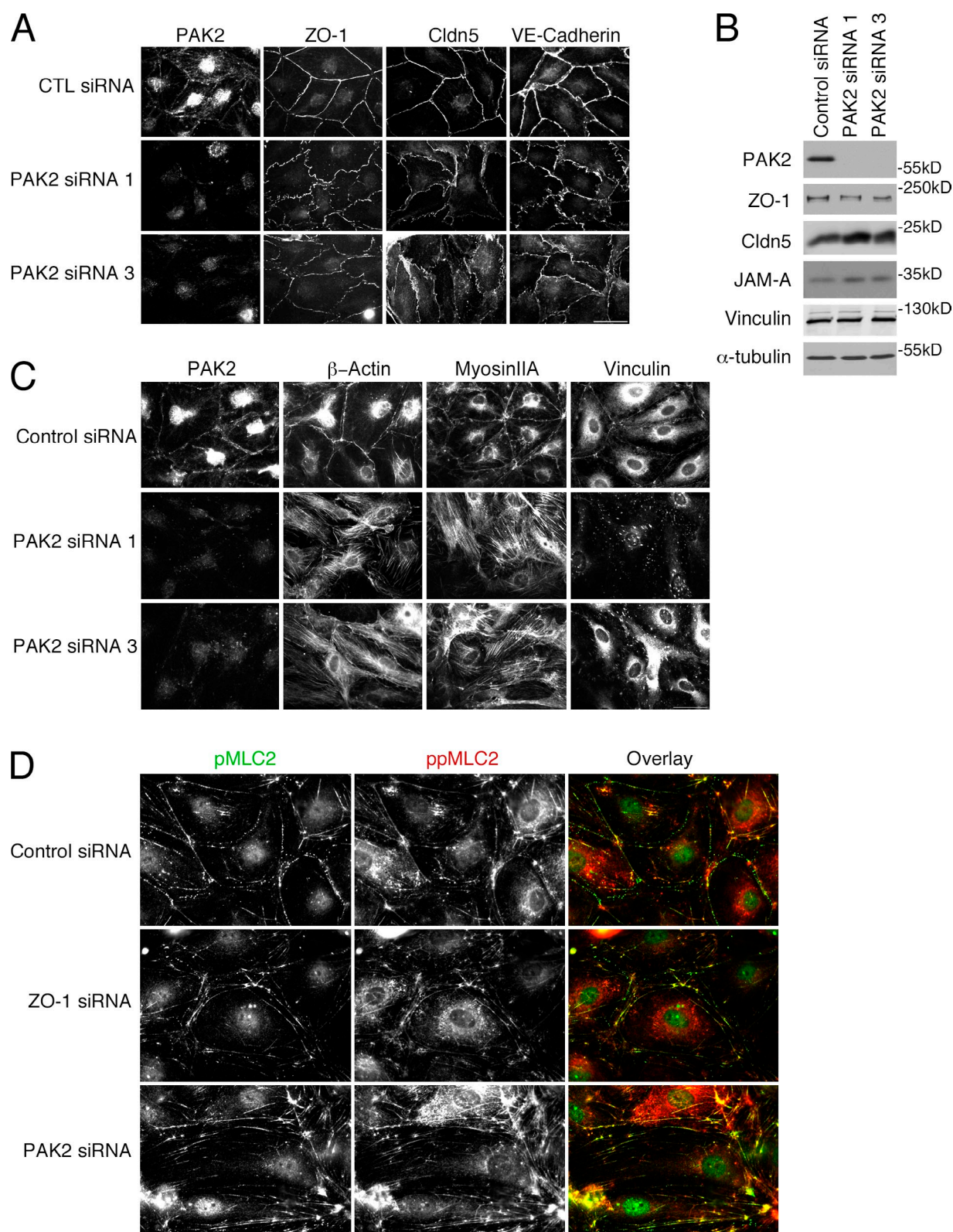


Figure 6. PAK2 down-regulation stimulates reorganization of the cytoskeleton. Cells transfected with control or two different PAK2 siRNAs were analyzed by immunofluorescence (A, C, and D) or immunoblotting as indicated (B). Results shown are representative from three duplicate experiments. Bars, 30 μ m.

ZO-1 regulates RhoA/ROCK by junctional recruitment of JACOP and p114RhoGEF

We next asked whether the link between ZO-1 and actomyosin might involve Rho signaling regulators. The RhoA activator

p114RhoGEF drives junctional myosin activation in epithelial cells by forming a complex with ROCK-II and myosin (Terry et al., 2011, 2012). It is recruited to epithelial tight junctions by cingulin; however, HDMEC express only low amounts of

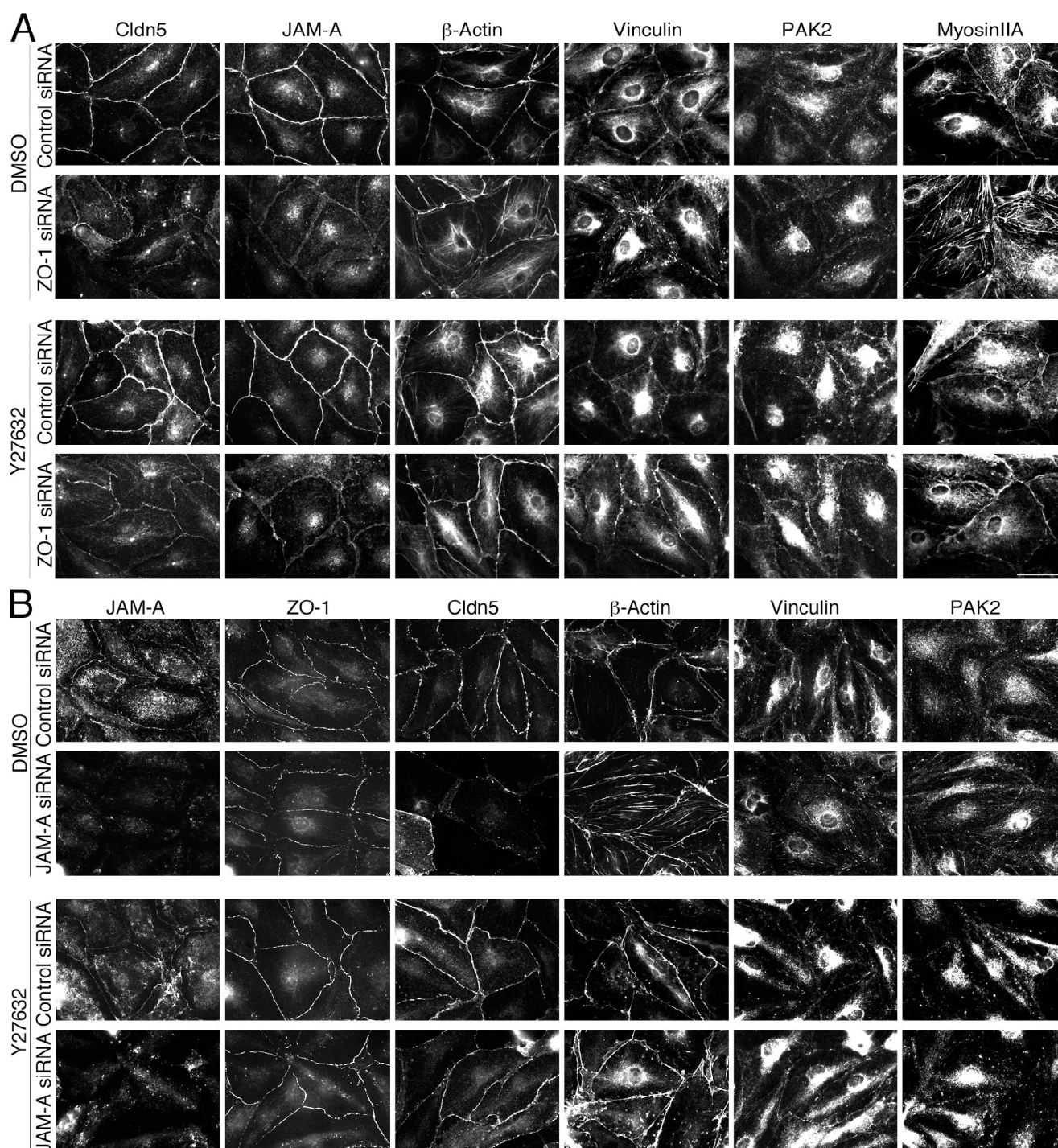


Figure 7. ROCK inhibition rescues the effects of ZO-1 or JAM-A depletion. Cells were transfected with control or ZO-1 siRNAs (A) or control and JAM-A siRNAs (B), and 48 h later were incubated for 24 h in the presence or absence of the ROCK inhibitor Y27632 (10 μ M). Then, the cells were fixed and analyzed by immunofluorescence for the indicated proteins (A). Results shown are representative from three duplicate experiments. Bars, 40 μ m.

cingulin, heterogeneously (unpublished data). A cingulin-like protein has been identified, JACOP/paracingulin, and the two proteins seem to have overlapping functions (Ohnishi et al., 2004; Citi et al., 2012).

Anti-JACOP antibodies stained HDMEC tight junctions strongly, and depletion of the protein resulted in a loss of junctional staining (Fig. 9, A and B). However, ZO-1 was still recruited to tight junctions. In contrast, ZO-1 depletion also led to

a redistribution of JACOP, which shifted to stress fibers along the central basal membrane and with structures along the periphery distinct from cell–cell contacts (Fig. 9 B). JACOP, but not vinculin, coimmunoprecipitated with ZO-1, which indicates that JACOP and ZO-1 form a complex (Fig. 9 C). Hence, ZO-1 mediates tight junction recruitment of JACOP in EC. Moreover, ZO-1 depletion also led to reduced recruitment of p190RhoGAP to adherens junctions, a protein known to be involved in the

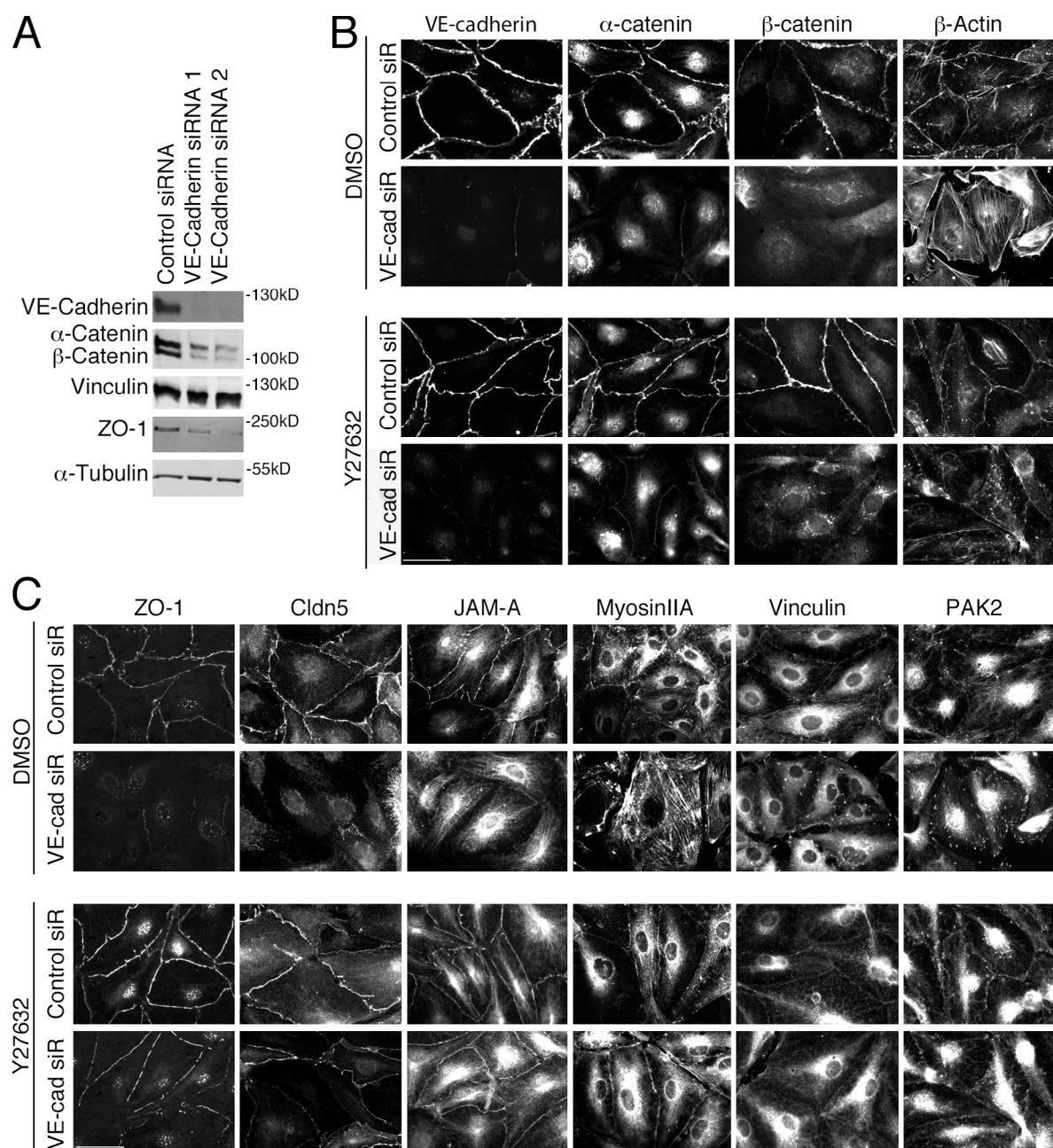


Figure 8. ROCK inhibition rescues the effects on the actin cytoskeleton and tight junctions of VE-cadherin down-regulation. (A) HDMEC transfected with the indicated siRNAs were analyzed by immunoblotting as labeled. Cells were transfected with control or VE-cadherin siRNAs and, 48 h later, were incubated for another 24 h in the presence or absence of the ROCK inhibitor Y27632. (B and C) Then, they were analyzed by immunofluorescence for the indicated proteins. Results shown are representative from three duplicate experiments. Bars: (B) 30 μ m; (C) 40 μ m.

down-regulation of RhoA signaling in response to cadherin ligation (Fig. S4). Strikingly, JACOP depletion also stimulated a redistribution of vinculin from junctions to focal adhesions and induction of stress fibers, which suggests that JACOP links ZO-1 to the regulation of the actomyosin system (Fig. 9 B).

In epithelial cells, cingulin can recruit p114RhoGEF to tight junctions (Terry et al., 2011). As cingulin and JACOP are homologous proteins, we asked whether JACOP associates with p114RhoGEF. Indeed, p114RhoGEF and JACOP coimmunoprecipitated from endothelial cell extracts, and both

ZO-1 and JACOP were required for junctional recruitment of p114RhoGEF (Fig. 9, B and E). Although JACOP coimmunoprecipitated with ZO-1, we were unable to detect ZO-1 in p114RhoGEF precipitates. Hence, it seems unlikely that the three proteins form a stable junction-associated heterotrimeric complex, but recruitment of the GEF may involve transient interactions. This is further supported by the observation that p114RhoGEF, and not ZO-1, immunoprecipitates contained vinculin (Fig. 9, C and E). Nevertheless, p114RhoGEF depletion led to a loss of junctional vinculin and induction of vinculin-stained focal adhesions and stress fibers comparable to

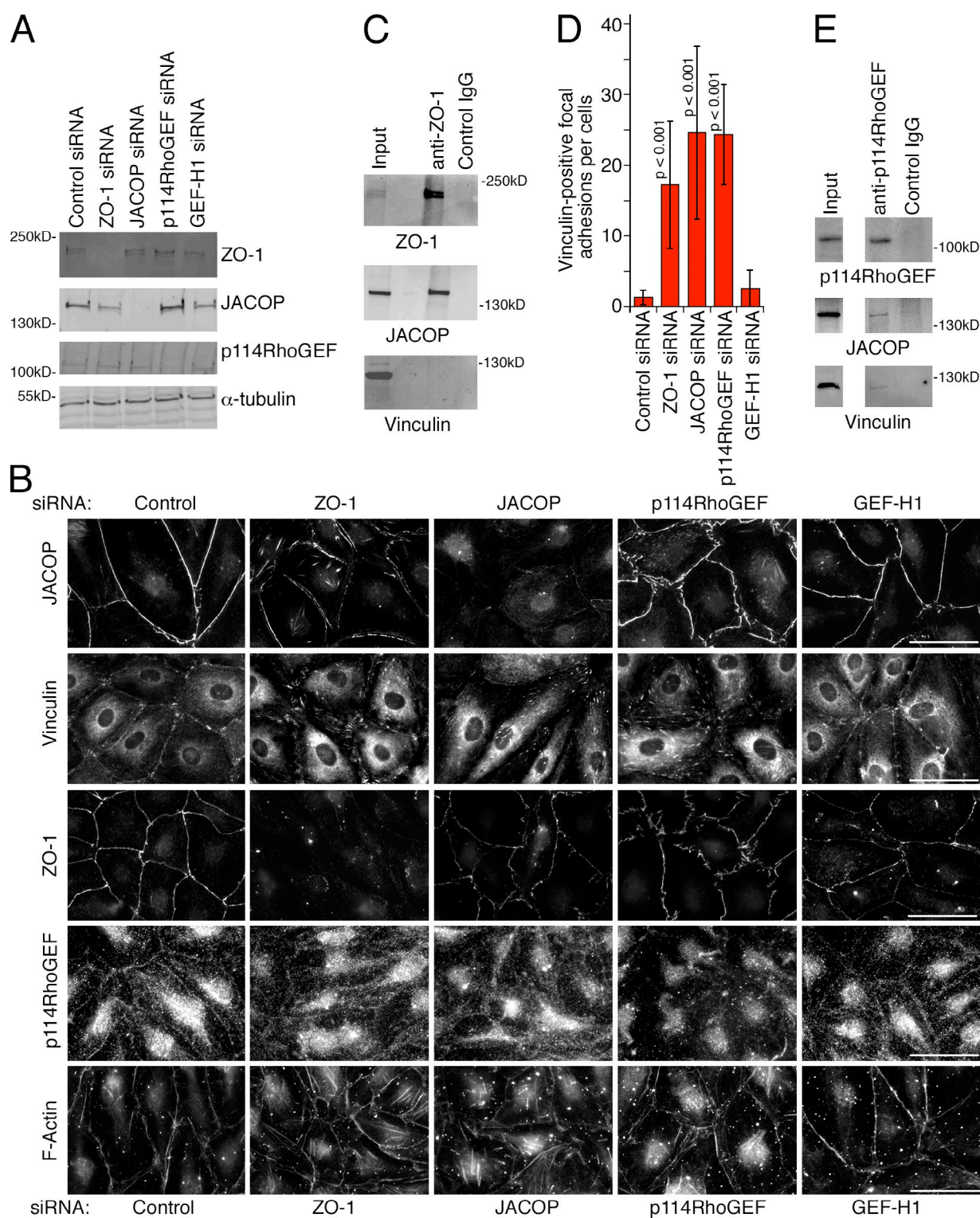


Figure 9. ZO-1 is required for junctional recruitment of JACOP and p114RhoGEF. (A and B) HDMEC were transfected as indicated with siRNAs and were then analyzed by immunoblotting (A) or immunofluorescence (B). (C) HDMEC were extracted and subjected to immunoprecipitation with anti-ZO-1 antibodies. The precipitates were then analyzed by immunoblotting for ZO-1, JACOP, and vinculin. (D) The number of vinculin-positive focal adhesions per cell were counted in images such as those shown in B. Shown are means \pm 1 SD (error bars); $n = 15$. (E) HDMEC were extracted and p114RhoGEF was immunoprecipitated. Precipitates were analyzed by immunoblotting for JACOP and vinculin. Bars, 30 μ m.

depletions of ZO-1 and JACOP (Fig. 9, B and D; and Fig. S5). In contrast, depletion of GEF-H1, which also binds JACOP and is inactive at tight junctions, did not reduce vinculin staining

and did not induce stress fibers. These data thus indicate that p114RhoGEF is recruited to endothelial junctions by ZO-1 and JACOP to stimulate junctional actomyosin activation and,

thereby, to ensure coupling of mechanotransducers to the VE-cadherin complex.

The observation that ROCK inhibition reverses the phenotype of ZO-1–depleted cells indicates an involvement of myosin activity. Hence, we added the myosin inhibitor Blebbistatin to siRNA-transfected cells and tested for F-actin and JAM-A redistribution. Blebbistatin-treated cells all had the same phenotype irrespective of whether control, ZO-1, or p114RhoGEF siRNAs were transfected. Both the F-actin and the JAM-A staining junctions had a wavy appearance but remained assembled, and stress fibers were not induced, which indicates that myosin activity is indeed required for the phenotype of ZO-1– or p114RhoGEF-depleted cells (Fig. 10, A and B). Inhibition of actin polymerization using CK666, an inhibitor of the Arp2/3 complex, or SMIFH2, a formin inhibitor, did not prevent induction of the ZO-1 or p114RhoGEF depletion phenotype (Fig. 10, A and B). Hence, junction dissociation in ZO-1– or p114RhoGEF-depleted cells requires ROCK and myosin activity.

Given the role of the actomyosin system in junction assembly, one would assume that the effect of ZO-1 depletion differs if depleted cells have not formed fully mature junctions. Hence, we repeated the siRNA experiments with cells plated at low density. Depletion of ZO-1 or p114RhoGEF in low-density cells led a striking actomyosin reorganization, and cells revealed gaps in between each other similar to control cells that had not started to form linear junctions (Fig. 10 C). Even the distribution of VE-cadherin itself was affected, as the protein was only detected in spot-like cell–cell contacts rather than linear junctions in depleted cells (Fig. 10 D). As observed for tight junction proteins at normal cell density, inhibition of ROCK resulted in the formation of linear VE-cadherin staining in control and depleted cells. In cells free of cell–cell contacts, depletion of either of the two proteins did not have any detectable effect, as expected if they normally function at cell–cell contacts. These observations thus further support the conclusion that ZO-1 directs the spatial actomyosin organization in endothelia to regulate junction assembly and integrity.

Discussion

Endothelial tight junctions are essential components of the vascular permeability barrier. Tight junctions are thought to be regulated by cadherin signaling, but have not been known to regulate adherens junctions. Here, we show that the tight junction adaptor protein ZO-1 is, in contrast to epithelia, essential for barrier formation in human microvascular EC and that it regulates cadherin-mediated cell–cell tension and cytoskeletal organization, as well as angiogenic potential and cell migration. ZO-1 functions as a major cytoskeletal organizer in EC, and not only determines the overall distribution of F-actin but also the recruitment of force-stimulating junctional proteins and force-transmitting cytoskeletal linkers to VE-cadherin complexes, and, hence, the tensile force acting on adherens junctions. Tight junctions can thus regulate adherens junctions.

ZO-1 deficiency in mice has been shown to induce defects in blood vessels in the yolk sac, with altered vascular trees associated with mislocalization of JAM-A (Katsuno et al., 2008).

However, the underlying molecular and cellular mechanisms for this defect were not known. Moreover, the effect on permeability is not clear in that model, as yolk sac vessels were already permeable to the tracer used in wild-type animals. The effect of ZO-1 deficiency in epithelial cells depends on the experimental conditions and, in terms of junction formation, ZO-1 and ZO-2 seem to have redundant functions. In Eph4 mammary epithelial and F9 cells, the combined deficiency of ZO-1 and -2 was shown to result in loss of tight junctions, and formation of adherens junctions positive for E-cadherin and reorganized F-actin but negative for myosin-II (Yamazaki et al., 2008). In contrast, in MDCK cells, depletion of ZO-1 and ZO-2 was reported to lead to an expansion of the perijunctional actomyosin ring associated with adherens junctions and apical constriction (Fanning et al., 2012). There is at present no explanation for these striking differences. Furthermore, ARHGEF11 has also been identified as a ZO-1–binding regulator of junction-associated actomyosin in mammary epithelial cells, but only the simultaneous knockdown of ARHGEF11 and ZO-2 resulted in significant impairment of TJs and of the perijunctional actomyosin ring, similar to when both ZO-1 and ZO-2 were depleted (Itoh et al., 2012). In contrast, p114RhoGEF can affect epithelial junction assembly without depletion of other junctional proteins (Terry et al., 2011). In our experiments with HDMEC, depletion of ZO-1 or p114RhoGEF alone was sufficient to induce a dramatic reorganization of the actomyosin cytoskeleton. Unlike any analyzed epithelial model, ZO-1 depletion induced increased myosin activation along the basal cell membrane and stress fiber formation. HDMEC express ZO-2, which was not affected by ZO-1 depletion, indicating that the two proteins are not redundant in EC. Moreover, our ROCK inhibition experiments suggest that the contradictory phenotypes observed in epithelia might have been caused by differential tension generated at cell–matrix adhesion sites in different epithelial model systems. In polarized simple epithelial cells, adherens and tight junctions are spatially well-separated at the apical aspect of the lateral plasma membrane. However, in EC, this topological separation is not well-defined, which might be the reason for the more general importance of ZO-1 for junction assembly. Nevertheless, whether the role of ZO-1 depends on the differential topology of the junctional complexes between epithelial cells and EC will need further analysis.

Adherens junctions in EC and epithelial cells are thought to be central bearers of tensile forces that are important for the regulation of tissue development, homeostasis, and function (Xiao et al., 2003; Birdsey et al., 2008; Hoffman et al., 2011; Yonemura, 2011; Conway et al., 2013; Huvneers and de Rooij, 2013). Although it is clear that the forces are generated by myosin motors and are transmitted by tension-sensitive linkers such as vinculin, it is still poorly understood how the signaling pathways that lead to the spatial regulation of these forces are orchestrated. Our data demonstrate that ZO-1 is one such regulator in primary EC that is essential for the maintenance of tensile forces on adherens junctions. Depletion of ZO-1 did not affect assembly of the core VE-cadherin complex; however, vinculin and myosin II were no longer associated with the complex, providing a molecular explanation for the reduced tensile forces.

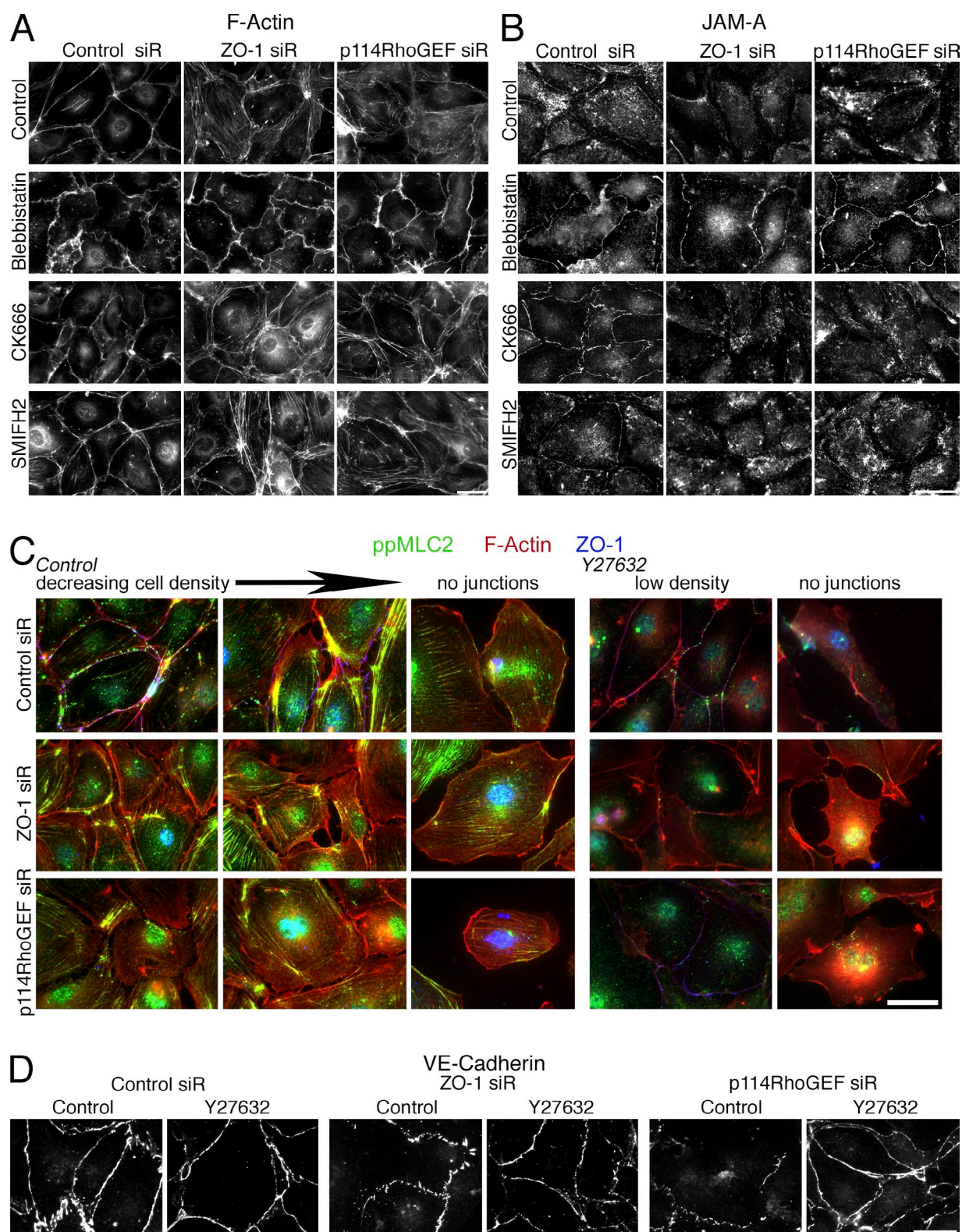


Figure 10. Regulation of cytoskeletal organization and junction assembly in low-density cultures. (A and B) HDMEC cells were transfected with siRNAs as indicated and then incubated with Blebbistatin, CK666, or SMIFH2 for the last 24 h before fixation. The cells were then stained for F-actin to visualize cytoskeletal organization (A) or JAM-A to monitor junction assembly (B). (C and D) Cells were plated at low density and then transfected with siRNAs. Before reaching full confluence, the cells were fixed and stained as indicated. Shown are images of areas where cells were already confluent or partially confluent, and images of cells without or with only little cell–cell contact. If indicated, the cells were incubated with the ROCK inhibitor Y27632 for 24 h before fixation. Bars, 20 μ m.

Moreover, our data further indicate that the balance between junctional and basal actomyosin activity is a crucial determinant of junction assembly, as inhibition of ROCK or myosin was sufficient to rescue recruitment of tight junction proteins.

VE-cadherin regulates cytoskeletal tension, cell spreading, and focal adhesions by stimulating RhoA (Xiao et al., 2003; Huveneers and de Rooij, 2013), and myosin II is the main force-generating actin motor. Hence, ZO-1 regulates the functional coupling of VE-cadherin to the force-generating machinery. Inhibition of myosin counteracted the redistribution of myosin and vinculin, indicating that it is the balance of forces between focal adhesions and the junctional complex that is important for junction assembly, and not force as such. Inhibition of ROCK not only affected the cytoskeleton but also reversed the redistribution of junctional claudin-5 and JAM-A, indicating that the maintenance of junctional tension is a main function of ZO-1.

Our data indicate that ZO-1 activates multiple pathways crucial for endothelial junction homeostasis. Junctional tension is clearly regulated by the actomyosin cytoskeleton, and ZO-1 depletion led to the deregulation of two pathways that can affect the activity of the actomyosin cytoskeleton. ZO-1 depletion led to loss of junctional PAK2, and depletion of the kinase was sufficient to recapitulate the redistribution of cytoskeletal proteins. However, PAK2 was not important for junctional recruitment of claudin-5; and depletion of claudin-5 was sufficient to disrupt the endothelial barrier, but did not affect actomyosin-driven processes such as migration. Hence, PAK2 and claudin-5 represent two distinct pathways regulated by ZO-1. In contrast, inhibition of ROCK led to a recovery of junctional claudin-5 in ZO-1-depleted cells, as well as to a recovery of junctional recruitment of PAK2 and components of the actomyosin cytoskeleton. Therefore, these results indicate that ZO-1's main role in junction assembly is the maintenance of junctional tension by promoting myosin activation through a pathway involving ROCK and, thereby, integrating different pathways to coordinate junction homeostasis and regulation.

Our data indicate that JACOP and p114RhoGEF are major components of the junctional ROCK signaling mechanism activated by ZO-1. ZO-1 forms a complex with JACOP, and both proteins are required for the junctional recruitment of p114RhoGEF. In mouse cardiac myocytes, ZO-1 was shown to bind vinculin directly (Zemljic-Harpf et al., 2014); however, we were unable to detect such vinculin–ZO-1 complexes in EC, and vinculin could be recruited to junctions in the absence of ZO-1 when ROCK was inhibited. Moreover, our data suggest that p114RhoGEF and JACOP are part of a biochemical complex that also contains vinculin but not ZO-1. As ZO-1 can bind JACOP directly (Citi et al., 2012), it might serve as a platform for the junctional recruitment of JACOP, which then forms complexes with other components such as p114RhoGEF and vinculin to regulate and mediate mechanotransduction.

Claudin-5 and JAM-A are major partners of ZO-1 in EC. Both transmembrane proteins have previously been shown to interact with ZO-1 directly (Bazzoni et al., 2000; Ebnet et al., 2000; Ooshio et al., 2010; Nomme et al., 2011). Based on our depletion data, the function of JAM-A closely mirrors that of ZO-1, which suggests that the two proteins cooperate. JAM-A

has been linked to the regulation of paracellular permeability, cell polarity, adhesion, migration, and angiogenesis, which has been linked to FGF-2 and integrin signaling (Nehls and Drenckhahn, 1995; Naik and Naik, 2008; Gutwein et al., 2009; Severson et al., 2009; Peddibhotla et al., 2013). Here, we demonstrate that JAM-A down-regulation in primary EC induces formation of actin/myosin II stress fibers and redistribution of vinculin and PAK2 from adherens junction to focal adhesions, similarly to ZO-1. ZO-1-depleted cells showed reduced angiogenic potential in VEGF-, FGF-2-, and IGF-containing media in vitro and in FGF-2-induced angiogenesis in vivo in plug assays. As JAM-A is known to regulate angiogenesis (Peddibhotla et al., 2013). This indicates that the cooperation of ZO-1 and JAM-A in EC is not only relevant for barrier formation but also for dynamic cellular processes such as angiogenesis, and is likely due to the deregulation of the actomyosin cytoskeleton and, hence, the spatial tension distribution.

Depletion of ZO-1 or JAM-A led to a redistribution of junctional claudin-5. Junctional accumulation could be recovered by inhibition of ROCK, which suggests that the distribution of tensile forces regulates claudin-5 accumulation at cell junctions (but not expression levels). As ROCKs have been shown to phosphorylate claudin-5, differential claudin phosphorylation may also contribute to the regulation of junctional recruitment (Yamamoto et al., 2008). ZO-1 also affects claudin-5 expression via a posttranscriptional mechanism, as mRNA levels were not affected by ZO-1 depletion (unpublished data). However, inhibition of lysosome function with chloroquine partially reversed the claudin-5 expression levels, which suggests that reduced expression was due to degradation upon disruption of tight junctions.

In summary, ZO-1 is a central regulator of intercellular junctions in EC that orchestrates the spatial organization of actomyosin activity, and thereby regulates junctional tension and linkage of VE-cadherin junctions to the force-generating machinery, recruitment of tight junction proteins and barrier formation, and endothelial cell dynamics. Our data indicate that ZO-1 and JAM-A form a cooperative unit that functions as a master regulator of endothelial tight junctions that stimulates junctional actomyosin activation via JACOP and p114RhoGEF, and thereby regulates endothelial barrier formation, cell–cell tension, and angiogenic potential by recruitment of additional actomyosin regulators, such as vinculin and PAK2.

Materials and methods

Cell culture, RNAi, and transfection

Human dermal microvascular EC (HDMEC-c adult C-12212) were obtained from PromoCell, maintained plated on 0.5% gelatin (G1393; Sigma-Aldrich)-coated tissue-culture Petri dishes in endothelial cell growth Medium MV2, and supplemented with C-39225 supplement mix (PromoCell). Cells were used between passage two and four. The following sequences were targeted with siRNAs: human ZO-1, 5'-GCAAAGACAUUGAUAGAAA-3' and 5'-CAAAAGAUUCGCAUCCUUA-3'; mouse ZO-1, 5'-UAACGGAGUUCAUUGGAU-3' and 5'-GUAGGAGAUUCAUUCUAUA-3'; Cldn5, 5'-CAAGAAGAACUACGUCUGA-3', 5'-CAUUGUCGUCGCGAGUUU-3', and 5'-UGGCGUUCGUUGCGCUCUU-3'; JAM-A, 5'-GCCUUUUU-GUCUUCUACA-3' and 5'-GAUAGUGAUGCCUACGAU-3'; PAK2, 5'-GGAUUUUCUAAAUCGAUGU-3' and 5'-GACAUUUGGUCUCUGGUA-3'; and VE-Cadherin, 5'-GUGGAUUACGACUCCUUA-3' and

5'-GGUAUGAGAUCGUGGUGGA-3'. The siRNAs for GEF-H1 (5'-GG-ACAAGCCUUCAGUGGUA-3', 5'-CAACAUUGCUGGACAUUUC-3', 5'-GAAUUAAGAUGGAGUUGGA-3', and 5'-GUGCGGAGCAGAU-GUGUAA-3'), p114RhoGEF (5'-UCAGGCGCUUGAAAGUA-3' and 5'-GGACGCAACUCGGACCAU-3'), and JACOP (CGNL1, 5'-GCA-GGGAGCUCGCAGAAU-3', 5'-CGGAGUACCUGAUUGAAU-3', 5'-CGAGUAAAGUGCUGGAUGA-3', and 5'-GGGAGAAUACGA-CAGUUA-3') were as described previously (Terry et al., 2011, 2012; Elbediwy et al., 2012). Non-targeting control siRNAs were 5'-UGUUU-ACAUGUCGACUAA-3' and 5'-UGUUUACAUGUUGUGUGA-3'. All siRNAs were obtained from Thermo Fisher Scientific and Sigma-Aldrich. Depending on the experimental condition, HDMEC were plated in multi-well dishes (e.g., 30,000 cells per well in 48-well dishes on 10-mm coverglasses, previously treated with 0.8 mg/ml Matrigel or 140 mm NUNC plates; 500,000 cells). The following day, transfection of siRNAs was performed using Lipofectamine RNAmax (Life Technologies) according to the manufacturer's instructions using a final siRNA concentration of 20–80 nM in antibiotic-free media. 24 h later, the medium was replaced and the cells were collected after 2–3 d for immunofluorescence, Western blotting, or immunoprecipitation. For DNA transfection, plasmids were mixed with JetPei (Polyplus) and incubated with cells for 2 h. The GFP-tagged mouse ZO-1 cDNA was generously provided by J. Ikenouchi (Kyushu University, Fukuoka, Japan). The ROCK inhibitor Y27632 (R&D Systems) was used at a concentration of 10 μ M. Blebbistatin (100 μ M), CK666 (20 μ M), and SMIFH2 (25 μ M) were purchased from Tocris Bioscience. The inhibitors were added to the media as indicated for 24 h. Chloroquine (Sigma-Aldrich) was used at 100 μ M for 10 h as described previously (Xiao et al., 2003).

Immunofluorescence, protein analysis, and antibodies

Cells were fixed either with methanol at -20°C for 5 min, 95% ethanol for 10 min at -20°C , or with 3% PFA for 20 min at room temperature followed by 0.3% Triton X-100 permeabilization for 5 min. The cells were then incubated with indicated primary antibodies and labeled using secondary antibodies labeled with Cy3, Cy5, or Alexa Fluor 488 (Jackson ImmunoResearch Laboratories, Inc.), and nuclei were visualized using Hoechst 33258 (Sigma-Aldrich) as described previously (Sourisseau et al., 2006). Coverslips were mounted with ProLong Gold mounting medium (Invitrogen) and stored at 4°C . Images were collected with a fluorescent microscope (DMIRB; Leica) using a 63 \times /1.4 NA oil immersion objective lens with a camera (C4742-95; Hamamatsu Photonics) and simple PCI software (Hamamatsu Photonics), or an inverted microscope (Eclipse Ti-E; Nikon) using a 60 \times /1.4 NA oil immersion objective lens, a camera (CoolSNAP HQ2; Photometrics), and Nikon software. Brightness and contrast were adjusted with Photoshop CS4 software (Adobe). For immunoblotting of whole-cell lysates, the cells were washed twice with PBS, lysed in SDS-PAGE sample buffer, and denatured at 70°C for 10 min (Sourisseau et al., 2006). The samples were then homogenized with a 1-ml syringe and a 25- and 3/4-g needle before SDS-PAGE and blotting onto nitrocellulose membranes. The membranes were blocked with 5% defatted milk powder dissolved in PBS containing 0.1% Tween-20. The following primary antibodies were used: mouse anti-ZO-1 (Invitrogen), mouse anti- β -actin (Sigma-Aldrich), rabbit anti- α -Catenin (Sigma-Aldrich), rabbit anti- β -Catenin (Sigma-Aldrich), mouse anti-Talin (Sigma-Aldrich), rabbit anti-Claudin5 (Abnova), rabbit anti-FAK (Santa Cruz Biotechnology, Inc.), rabbit anti-pFAK (Y397; Invitrogen), rabbit anti-ILK (Cell Signaling Technology), mouse anti-JAM-A (Santa Cruz Biotechnology, Inc.), rabbit anti-JAM-A (Invitrogen), mouse anti-pMLC2 (19; Cell Signaling Technology), rabbit anti-ppMLC2 (18–19; Cell Signaling Technology), rabbit anti-MyosinIIA (Sigma-Aldrich), rabbit anti-PAK2 (Epitomics), rabbit anti-paxillin (Cell Signaling Technology), mouse anti-p120Catenin (BD), mouse anti-VE-Cadherin (BD), rabbit anti-VE-cadherin (AbD Serotec), mouse anti-Vinculin (Sigma-Aldrich), rabbit anti-JACOP (Sana Cruz Biotechnology, Inc.), and goat anti-p114RhoGEF (Everest Bio-tech Ltd.). A mouse anti- α -tubulin antibody was used that had been generated against the 11 C-terminal amino acids of porcine α -tubulin (Kreis, 1987). The rabbit anti-ZO-1 (antigen: the peptide N-YTDQELDETINDEV-C), anti-ZO-2 (antigen: the peptide N-KMEGMDDDPEDRMSC-C), and GEF-H1 (antigen: the peptide N-CDFRMQDIPETES-C) have been described previously (Benais-Pont et al., 2003). For coimmunoprecipitation, 500,000 HDMEC were seeded onto 140-mm NUNC cell culture dishes treated with 0.5% gelatin. Three dishes were used per immunoprecipitation. Cells were lysed and extracted with RIPA buffer (50 mM Tris, pH 7.5, 150 mM NaCl, 0.1% SDS, 0.5% sodium deoxycholate, and 1% Triton X-100) containing a cocktail of protease inhibitors (50 μ g/ml PMSF, 10 μ g/ml aprotinin, 10 μ g/ml leupeptin, and 10 μ g/ml pepstatin) at 4°C . The whole-cell lysates were

incubated with unconjugated Sepharose beads for 30 min at 4°C . The extracts were then spun for 10 min at 10,000 g in a cooled microcentrifuge, and the supernatants were loaded onto protein G-Sepharose that had been conjugated with a rabbit anti- α -Catenin antibody (Sigma-Aldrich), mouse anti-talin antibody (Sigma-Aldrich), or mouse anti-VE-cadherin antibody (BD). Corresponding negative controls were rabbit or mouse IgGs. After 3.5 h on a shaker at 4°C , the beads were washed with extraction buffer followed by PBS. Precipitates were then analyzed by immunoblotting.

Microcarrier-based fibrin gel angiogenesis assay

Gelatin-coated cytodex-3 MCs (Sigma-Aldrich) were suspended in PBS at 30% and autoclaved. MCs were washed with EMB-2 (Lonza) before being added to EC to a final density of 100 cells/MC. The day after the siRNA transfection, HDMEC were trypsinized and allowed to attach to the MCs in 1.5 ml of medium for 4 h at 37°C . The MCs were then resuspended and cultivated for another 24–48 h at 37°C in 1–2 wells of a 24-well dish (Thermo Fisher Scientific). HDMEC attached to MCs were used in fibrin gel angiogenesis assays as described previously (Nehls and Drenckhahn, 1995; Sun et al., 2004) with some modifications. Fibrinogen (Sigma-Aldrich) was prepared by diluting the stock solution of fibrinogen (20 mg/ml in PBS) in EBM-2 to a concentration of 1.7 mg/ml, supplemented with EGF (PeproTech EC Ltd) and hydrocortisone (Sigma-Aldrich) at 10 ng/ml and 1.0 μ g/ml, respectively. The 48-well plates were used for the assays, 200 μ l of fibrinogen solution containing \sim 150 HDMEC-coated MCs was added per well, and the clotting was induced by the addition of thrombin (0.5 U/ml). After 30 min of polymerization, 0.5 ml of EBM-2 supplemented with 10 ng/ml of EGF, 40 ng/ml of bFGF (PeproTech EC Ltd) and VEGF-165 (PeproTech EC Ltd), 1.0 μ g/ml of hydrocortisone, and 50 ml/liter adult human serum (Sigma-Aldrich) were layered on top of the gel. To prevent excess fibrinolysis by fibrin-embedded cells, aprotinin was added to the growth media at 200 KIU/ml for only the first day. The medium was replaced every 2 d and phase contrast pictures were taken after 4–5 d in fibrinogen culture. The cells were then fixed with 3% PFA and permeabilized with 1% Triton X-100 in PBS and 1% BSA to stain DNA with Hoechst 33258 dye and F-actin with Cy3-phalloidine for confirmation that MC beads were covered with cells.

Capillary-like formation on Matrigel and cell migration

Ice-cold Matrigel growth factor reduced (BD; 8–10 mg/ml, 50 μ l/well) was added to flat-bottom 96-well plates and allowed to solidify for 1 h at 37°C . HDMEC (15,000 cells/well) that had been transfected with siRNAs 48 h before were seeded in duplicate into the coated wells and incubated at 37°C in ECGMv2. Pictures were taken at different times and capillaries were fixed in phosphate-buffered formalin at the end of the experiment. Branching points were quantified in four different fields and two different experiments per conditions. For cell migration analysis, HDMEC were plated on 48-well dishes and RNAi was performed as described above. 40 h later, a wound was inflicted with a plastic yellow tip and pictures were taken. Cells were allowed to migrate at 37°C . Pictures were taken at different times using a 5 \times /0.12 NA objective lens on an inverted microscope (DMIRB; Leica), a camera (C4742-95; Hamamatsu Photonics), and simple PCI software (ambient temperature). The area without cells was calculated at the different times using ImageJ.

Endothelial permeability assay

HDMEC were seeded in 140-mm dishes, and transfected the following day with siRNAs. 24 h later, the cells were trypsinized and plated in Costar/Corning permeability inserts (6.5-mm diameter, 1.0- μ m pore size) precoated with Matrigel (0.8 mg/ml; 100,000 cells per insert; BD). After 24 h, transendothelial electrical resistance (TER) was determined using an epithelial volt ohm meter (EVOM). After another 24 h, a second determination of TER was performed and endothelial paracellular permeability was assayed by adding 4 and 70 kD FITC- and Rhodamine-conjugated dextran (1 mg/ml; Sigma-Aldrich), respectively, to the apical side. Permeability was determined by measuring the respective fluorescence intensity that was emitted from 50 μ l medium taken from the basolateral side using a fluorescence reader (BMG Labtech; Steed et al., 2009).

Apoptosis assay

HDMEC that had been transfected with siRNAs for 48 h were seeded onto 96-well plates pretreated with 0.8 mg Matrigel and incubated at 37°C in ECGMv2 for 24 h. Then, the total cell numbers were determined using Cy-Quant and an identical plate was analyzed for apoptosis by measuring caspase 3 and 7 activity using the Caspase-Glo 3/7 Assay (Promega) and

for necrosis by measuring lactate dehydrogenase release (Promega) as described previously (Nie et al., 2012).

FRET tension and Rho activity measurements

HDMEC were plated into coated 8-well multi-chamber ibidi slides (40,000 cells/well) and then transfected with siRNAs after 19 h. On day 3 after plating, the cells were transfected with plasmids encoding the VE-cadherin-based FRET tension sensors (Conway et al., 2013) or the RhoA biosensor (pRaichu-RhoA; Yoshizaki et al., 2003; Terry et al., 2011) using JetPei (Elbediwy et al., 2012). The transfection mixes were incubated with the cells for 2 h and then replaced with fresh medium. 20 h later, FRET was assessed using an SP2 microscope (Leica; 63×/1.4 NA objective lens, 37°C) and LCS FRET software (Leica) using the donor recovery after acceptor bleaching protocol and generating the shown FRET efficiency maps according to the equation $[(D_{\text{post}}D_{\text{pre}})/D_{\text{post}}] \times 100$ (where D represents donor intensity).

Matrigel plug angiogenesis assay

The Matrigel plug assay was performed and analyzed as described previously (Birdsey et al., 2008). In brief, C57BL/6 mice were injected with a mix of Matrigel (BD), heparin, and, depending on the condition, FGF, and 2 μM siRNAs near the abdominal midline. Plugs were harvested after 7 d from killed mice, fixed in 4% paraformaldehyde in PBS for 2 h at room temperature, transferred to 70% ethanol, embedded in paraffin, and processed for hematoxylin and eosin staining. For quantification, vessels contained in the Matrigel plug were identified by the presence of nucleated cells surrounding a lumen containing red blood cells. Vessels were counted in four fields of view using a 20× objective lens. For immunofluorescence, sections were dewaxed and antigen retrieval was performed in sodium citrate buffer (0.01 M, pH 6) in a microwave for 10 min. Images were acquired with an inverted microscope (Eclipse Ti-E; Nikon) using a 60×/1.4 NA oil immersion objective lens, a camera (CoolSnap HQ2; Photometrics), and Nikon software at ambient temperature. Experiments were performed according to the Animals (Scientific Procedures) Act of 1986.

Laser ablation experiments

HDMEC were labeled by transduction with a lentiviral vector encoding GFP-α-catenin (Huveneers et al., 2012). The cells were then seeded and transfected with siRNAs using ibidi 8-well multi-chamber slides. Ablation experiments were then performed at 37°C with an inverted microscope (Eclipse Ti-E; Nikon) equipped with a Micropoint Galvo system (Andor Technology) containing a pulsed N₂ laser. To enable observation of GFP and ablation at 404 nm, a beam splitter was used that allowed transmission of 70% of the laser light. The laser intensity was calibrated to allow ablation with the lowest energy required firing the laser once into the targeted cell (60–80% of the laser power depending on the age of the dye). All experiments were performed with a CFI Apochromat Nano-Crystal 60× oil objective lens (NA 1.2). Movies were made by recording 1 frame per second for 1 min and are shown playing 5 frames per second. Images collected just before ablation, and 30 s and 45 s after ablation, were used for analysis using ImageJ. The overlays in Fig. 2 show the starting image in red, 30 s in green, and 45 s in blue.

Online supplemental material

Fig. S1 shows the immunofluorescence of ZO-1 for control and ZO-1-depleted sections from Matrigel plug assays, the depletion of ZO-1 in mouse EC using different siRNAs, and endomucin staining of Matrigel plug sections. Fig. S2 shows the effect of ZO-1 depletion on claudin-5 expression, rescue of junctional vinculin upon mouse GFP-ZO-1 expression in human cells, and the effect of claudin-5 depletion on tight junction functions and in vitro angiogenesis. Fig. S3 shows the analysis of active RhoA localization in control and ZO-1-depleted cells. Fig. S4 shows the defect in junctional recruitment of p190RhoGAP in ZO-1-depleted cells. Fig. S5 shows the redistribution of active myosin IIA in response to down-regulation of ZO-1, JACOP, or p114RhoGEF. Online supplemental material is available at <http://www.jcb.org/cgi/content/full/jcb.201404140/DC1>.

This work was supported by the Medical Research Council (G0900098), the Wellcome Trust (099173/Z/12/Z), and the Biotechnology and Biological Sciences Research Council (BB/J015032/1 and BB/L007584/1). M.A. Schwartz was supported by National Institutes of Health grant RO1 HL75092.

The authors declare no competing financial interests.

Submitted: 25 April 2014

Accepted: 3 February 2015

References

- Bazzoni, G. 2011. Pathobiology of junctional adhesion molecules. *Antioxid. Redox Signal.* 15:1221–1234. <http://dx.doi.org/10.1089/ars.2010.3867>
- Bazzoni, G., O.M. Martinez-Estrada, F. Orsenigo, M. Cordenonsi, S. Citi, and E. Dejana. 2000. Interaction of junctional adhesion molecule with the tight junction components ZO-1, cingulin, and occludin. *J. Biol. Chem.* 275:20520–20526. <http://dx.doi.org/10.1074/jbc.M905251199>
- Benaïs-Pont, G., A. Punnett, C. Flores-Maldonado, J. Eckert, G. Raposo, T.P. Fleming, M. Cerejido, M.S. Balda, and K. Matter. 2003. Identification of a tight junction-associated guanine nucleotide exchange factor that activates Rho and regulates paracellular permeability. *J. Cell Biol.* 160:729–740. <http://dx.doi.org/10.1083/jcb.200211047>
- Birdsey, G.M., N.H. Dryden, V. Amselem, F. Gebhardt, K. Sahnun, D.O. Haskard, E. Dejana, J.C. Mason, and A.M. Randi. 2008. Transcription factor Erg regulates angiogenesis and endothelial apoptosis through VE-cadherin. *Blood.* 111:3498–3506. <http://dx.doi.org/10.1182/blood-2007-08-105346>
- Cavallaro, U., and E. Dejana. 2011. Adhesion molecule signalling: not always a sticky business. *Nat. Rev. Mol. Cell Biol.* 12:189–197. <http://dx.doi.org/10.1038/nrm3068>
- Citi, S., P. Pulimeno, and S. Paschoud. 2012. Cingulin, paracingulin, and PLEKHA7: signaling and cytoskeletal adaptors at the apical junctional complex. *Ann. NY Acad. Sci.* 1257:125–132. <http://dx.doi.org/10.1111/j.1749-6632.2012.06506.x>
- Conway, D., and M.A. Schwartz. 2012. Lessons from the endothelial junctional mechanosensory complex. *F1000 Biol. Rep.* 4:1.
- Conway, D.E., M.T. Breckenridge, E. Hinde, E. Gratton, C.S. Chen, and M.A. Schwartz. 2013. Fluid shear stress on endothelial cells modulates mechanical tension across VE-cadherin and PECAM-1. *Curr. Biol.* 23:1024–1030. <http://dx.doi.org/10.1016/j.cub.2013.04.049>
- Cooke, V.G., M.U. Naik, and U.P. Naik. 2006. Fibroblast growth factor-2 failed to induce angiogenesis in junctional adhesion molecule-A-deficient mice. *Arterioscler. Thromb. Vasc. Biol.* 26:2005–2011. <http://dx.doi.org/10.1161/01.ATV.0000234923.79173.99>
- Ebnet, K., C.U. Schulz, M.K. Meyer Zu Brickwedde, G.G. Pendl, and D. Vestweber. 2000. Junctional adhesion molecule interacts with the PDZ domain-containing proteins AF-6 and ZO-1. *J. Biol. Chem.* 275:27979–27988.
- Elbediwy, A., C. Zihni, S.J. Terry, P. Clark, K. Matter, and M.S. Balda. 2012. Epithelial junction formation requires confinement of Cdc42 activity by a novel SH3BP1 complex. *J. Cell Biol.* 198:677–693. <http://dx.doi.org/10.1083/jcb.201202094>
- Fanning, A.S., and J.M. Anderson. 2009. Zonula occludens-1 and -2 are cytosolic scaffolds that regulate the assembly of cellular junctions. *Ann. NY Acad. Sci.* 1165:113–120. <http://dx.doi.org/10.1111/j.1749-6632.2009.04440.x>
- Fanning, A.S., C.M. Van Itallie, and J.M. Anderson. 2012. Zonula occludens-1 and -2 regulate apical cell structure and the zonula adherens cytoskeleton in polarized epithelia. *Mol. Biol. Cell.* 23:577–590. <http://dx.doi.org/10.1091/mbc.E11-09-0791>
- Grashoff, C., B.D. Hoffman, M.D. Brenner, R. Zhou, M. Parsons, M.T. Yang, M.A. McLean, S.G. Sligar, C.S. Chen, T. Ha, and M.A. Schwartz. 2010. Measuring mechanical tension across vinculin reveals regulation of focal adhesion dynamics. *Nature.* 466:263–266. <http://dx.doi.org/10.1038/nature09198>
- Gutwein, P., A. Schramme, B. Voss, M.S. Abdel-Bakky, K. Doberstein, A. Ludwig, P. Altevogt, M.L. Hansmann, H. Moch, G. Kristiansen, and J. Pfeilschifter. 2009. Downregulation of junctional adhesion molecule-A is involved in the progression of clear cell renal cell carcinoma. *Biochem. Biophys. Res. Commun.* 380:387–391. <http://dx.doi.org/10.1016/j.bbrc.2009.01.100>
- Haskard, D.O., J.J. Boyle, P.C. Evans, J.C. Mason, and A.M. Randi. 2013. Cytoprotective signaling and gene expression in endothelial cells and macrophages—lessons for atherosclerosis. *Microcirculation.* 20:203–216. <http://dx.doi.org/10.1111/micc.12020>
- Hoffman, B.D., C. Grashoff, and M.A. Schwartz. 2011. Dynamic molecular processes mediate cellular mechanotransduction. *Nature.* 475:316–323. <http://dx.doi.org/10.1038/nature10316>
- Huveneers, S., and J. de Rooij. 2013. Mechanosensitive systems at the cadherin-F-actin interface. *J. Cell Sci.* 126:403–413. <http://dx.doi.org/10.1242/jcs.109447>
- Huveneers, S., J. Oldenburg, E. Spanjaard, G. van der Krogt, I. Grigoriev, A. Akhmanova, H. Rehmann, and J. de Rooij. 2012. Vinculin associates with endothelial VE-cadherin junctions to control force-dependent remodeling. *J. Cell Biol.* 196:641–652. <http://dx.doi.org/10.1083/jcb.201108120>
- Itoh, M., S. Tsukita, Y. Yamazaki, and H. Sugimoto. 2012. Rho GTP exchange factor ARHGAP11 regulates the integrity of epithelial junctions by connecting ZO-1 and RhoA-myosin II signaling. *Proc. Natl. Acad. Sci. USA.* 109:9905–9910. <http://dx.doi.org/10.1073/pnas.1115063109>

- Katsuno, T., K. Umeda, T. Matsui, M. Hata, A. Tamura, M. Itoh, K. Takeuchi, T. Fujimori, Y. Nabeshima, T. Noda, et al. 2008. Deficiency of zonula occludens-1 causes embryonic lethal phenotype associated with defected yolk sac angiogenesis and apoptosis of embryonic cells. *Mol. Biol. Cell.* 19:2465–2475. <http://dx.doi.org/10.1091/mbc.E07-12-1215>
- Kreis, T.E. 1987. Microtubules containing detyrosinated tubulin are less dynamic. *EMBO J.* 6:2597–2606.
- Lamagna, C., K.M. Hodivala-Dilke, B.A. Imhof, and M. Aurrand-Lions. 2005. Antibody against junctional adhesion molecule-C inhibits angiogenesis and tumor growth. *Cancer Res.* 65:5703–5710. <http://dx.doi.org/10.1158/0008-5472.CAN-04-4012>
- Lampugnani, M.G. 2012. Endothelial cell-to-cell junctions: adhesion and signaling in physiology and pathology. *Cold Spring Harb. Perspect. Med.* 2:a006528. <http://dx.doi.org/10.1101/cshperspect.a006528>
- Martin, T.A. 2014. The role of tight junctions in cancer metastasis. *Semin. Cell Dev. Biol.* 36:224–231. <http://dx.doi.org/10.1016/j.semcdb.2014.09.008>
- Naik, U.P., and M.U. Naik. 2008. Putting the brakes on cancer cell migration: JAM-A restrains integrin activation. *Cell Adhes. Migr.* 2:249–251. <http://dx.doi.org/10.4161/cam.2.4.6753>
- Nehls, V., and D. Drenckhahn. 1995. A novel, microcarrier-based in vitro assay for rapid and reliable quantification of three-dimensional cell migration and angiogenesis. *Microvasc. Res.* 50:311–322. <http://dx.doi.org/10.1006/mvre.1995.1061>
- Nie, M., M.S. Balda, and K. Matter. 2012. Stress- and Rho-activated ZO-1-associated nucleic acid binding protein binding to p21 mRNA mediates stabilization, translation, and cell survival. *Proc. Natl. Acad. Sci. USA.* 109:10897–10902. <http://dx.doi.org/10.1073/pnas.1118822109>
- Nitta, T., M. Hata, S. Gotoh, Y. Seo, H. Sasaki, N. Hashimoto, M. Furuse, and S. Tsukita. 2003. Size-selective loosening of the blood-brain barrier in claudin-5-deficient mice. *J. Cell Biol.* 161:653–660. <http://dx.doi.org/10.1083/jcb.200302070>
- Nomme, J., A.S. Fanning, M. Caffrey, M.F. Lye, J.M. Anderson, and A. Lavie. 2011. The Src homology 3 domain is required for junctional adhesion molecule binding to the third PDZ domain of the scaffolding protein ZO-1. *J. Biol. Chem.* 286:43352–43360. <http://dx.doi.org/10.1074/jbc.M111.304089>
- Ohnishi, H., T. Nakahara, K. Furuse, H. Sasaki, S. Tsukita, and M. Furuse. 2004. JACOP, a novel plaque protein localizing at the apical junctional complex with sequence similarity to cingulin. *J. Biol. Chem.* 279:46014–46022. <http://dx.doi.org/10.1074/jbc.M402616200>
- Ooshio, T., R. Kobayashi, W. Ikeda, M. Miyata, Y. Fukumoto, N. Matsuzawa, H. Ogita, and Y. Takai. 2010. Involvement of the interaction of afadin with ZO-1 in the formation of tight junctions in Madin-Darby canine kidney cells. *J. Biol. Chem.* 285:5003–5012. <http://dx.doi.org/10.1074/jbc.M109.043760>
- Peddibhotla, S.S., B.F. Brinkmann, D. Kummer, H. Tuncay, M. Nakayama, R.H. Adams, V. Gerke, and K. Ebnet. 2013. Tetraspanin CD9 links junctional adhesion molecule-A to $\alpha\beta 3$ integrin to mediate basic fibroblast growth factor-specific angiogenic signaling. *Mol. Biol. Cell.* 24:933–944. <http://dx.doi.org/10.1091/mbc.E12-06-0481>
- Pulimeno, P., S. Paschoud, and S. Citi. 2011. A role for ZO-1 and PLEKHA7 in recruiting paracatulin to tight and adherens junctions of epithelial cells. *J. Biol. Chem.* 286:16743–16750. <http://dx.doi.org/10.1074/jbc.M111.230862>
- Severson, E.A., W.Y. Lee, C.T. Capaldo, A. Nusrat, and C.A. Parkos. 2009. Junctional adhesion molecule A interacts with Afadin and PDZ-GEF2 to activate Rap1A, regulate $\beta 1$ integrin levels, and enhance cell migration. *Mol. Biol. Cell.* 20:1916–1925. <http://dx.doi.org/10.1091/mbc.E08-10-1014>
- Sourisseau, T., A. Georgiadis, A. Tsapara, R.R. Ali, R. Pestell, K. Matter, and M.S. Balda. 2006. Regulation of PCNA and cyclin D1 expression and epithelial morphogenesis by the ZO-1-regulated transcription factor ZONAB/DbpA. *Mol. Cell. Biol.* 26:2387–2398. <http://dx.doi.org/10.1128/MCB.26.6.2387-2398.2006>
- Steed, E., N.T. Rodrigues, M.S. Balda, and K. Matter. 2009. Identification of MarvelD3 as a tight junction-associated transmembrane protein of the occludin family. *BMC Cell Biol.* 10:95. <http://dx.doi.org/10.1186/1471-2121-10-95>
- Stockton, R.A., E. Schaefer, and M.A. Schwartz. 2004. p21-activated kinase regulates endothelial permeability through modulation of contractility. *J. Biol. Chem.* 279:46621–46630. <http://dx.doi.org/10.1074/jbc.M408877200>
- Sun, X.T., Y.T. Ding, X.G. Yan, L.Y. Wu, Q. Li, N. Cheng, Y.D. Qiu, and M.Y. Zhang. 2004. Angiogenic synergistic effect of basic fibroblast growth factor and vascular endothelial growth factor in an in vitro quantitative microcarrier-based three-dimensional fibrin angiogenesis system. *World J. Gastroenterol.* 10:2524–2528.
- Terry, S.J., C. Zihni, A. Elbediwy, E. Vitiello, I.V. Leefa Chong San, M.S. Balda, and K. Matter. 2011. Spatially restricted activation of RhoA signalling at epithelial junctions by p114RhoGEF drives junction formation and morphogenesis. *Nat. Cell Biol.* 13:159–166. <http://dx.doi.org/10.1038/ncb2156>
- Terry, S.J., A. Elbediwy, C. Zihni, A.R. Harris, M. Bailly, G.T. Charras, M.S. Balda, and K. Matter. 2012. Stimulation of cortical myosin phosphorylation by p114RhoGEF drives cell migration and tumor cell invasion. *PLoS ONE.* 7:e50188. <http://dx.doi.org/10.1371/journal.pone.0050188>
- Van Itallie, C.M., A.S. Fanning, A. Bridges, and J.M. Anderson. 2009. ZO-1 stabilizes the tight junction solute barrier through coupling to the perijunctional cytoskeleton. *Mol. Biol. Cell.* 20:3930–3940. <http://dx.doi.org/10.1091/mbc.E09-04-0320>
- Weber, C., L. Fraemohs, and E. Dejana. 2007. The role of junctional adhesion molecules in vascular inflammation. *Nat. Rev. Immunol.* 7:467–477. <http://dx.doi.org/10.1038/nri2096>
- Xiao, K., D.F. Allison, M.D. Kottke, S. Summers, G.P. Sorescu, V. Faundez, and A.P. Kowalczyk. 2003. Mechanisms of VE-cadherin processing and degradation in microvascular endothelial cells. *J. Biol. Chem.* 278:19199–19208. <http://dx.doi.org/10.1074/jbc.M211746200>
- Yamamoto, M., S.H. Ramirez, S. Sato, T. Kiyota, R.L. Cerny, K. Kaibuchi, Y. Persidsky, and T. Ikezu. 2008. Phosphorylation of claudin-5 and occludin by rho kinase in brain endothelial cells. *Am. J. Pathol.* 172:521–533. <http://dx.doi.org/10.2353/ajpath.2008.070076>
- Yamazaki, Y., K. Umeda, M. Wada, S. Nada, M. Okada, S. Tsukita, and S. Tsukita. 2008. ZO-1- and ZO-2-dependent integration of myosin-2 to epithelial zonula adherens. *Mol. Biol. Cell.* 19:3801–3811. <http://dx.doi.org/10.1091/mbc.E08-04-0352>
- Yonemura, S. 2011. A mechanism of mechanotransduction at the cell-cell interface: emergence of α -catenin as the center of a force-balancing mechanism for morphogenesis in multicellular organisms. *BioEssays.* 33:732–736. <http://dx.doi.org/10.1002/bies.201100064>
- Yonemura, S., Y. Wada, T. Watanabe, A. Nagafuchi, and M. Shibata. 2010. α -Catenin as a tension transducer that induces adherens junction development. *Nat. Cell Biol.* 12:533–542. <http://dx.doi.org/10.1038/ncb2055>
- Yoshizaki, H., Y. Ohba, K. Kurokawa, R.E. Itoh, T. Nakamura, N. Mochizuki, K. Nagashima, and M. Matsuda. 2003. Activity of Rho-family GTPases during cell division as visualized with FRET-based probes. *J. Cell Biol.* 162:223–232. <http://dx.doi.org/10.1083/jcb.200212049>
- Zemljic-Harpf, A.E., J.C. Godoy, O. Platoshyn, E.K. Asfaw, A.R. Busija, A.A. Domenighetti, and R.S. Ross. 2014. Vinculin directly binds zonula occludens-1 and is essential for stabilizing connexin-43-containing gap junctions in cardiac myocytes. *J. Cell Sci.* 127:1104–1116. <http://dx.doi.org/10.1242/jcs.143743>